DISSOLUTION RATE EQUATIONS IN COLUMN CONFINED DISSOLUTION

by

KAILASH C. DHUPAR

A thesis submitted in partial fulfillment of the requirements for the degree of

MASTER OF SCIENCE

Pharmacy
(Pharmaceutics)

at the

UNIVERSITY OF WISCONSIN

1975

Approval Sheet

Dissolution Rate Equations in Column Confined Dissolution

Kailash C. Dhupar

Master's Thesis

This Thesis is Approved:

J.T. Carstensen

J.T.Carstensen, Major Professor

George Zografi

George Zografi

Gordon L. Amidon

Gordon L. Amidon

Peter G. Welling

Peter G. Welling

TO

My wife, Shanti,
my mother & family
for their love,
encouragement and
understanding.

ACKNOWLEDGEMENTS

I wish to express my sincere gratitude to Professor Jens T.Carstensen for his guidance during the course of this study. It has been a key source of motivation. His encouragements and his interest has had a big influence on my graduate career.

I am also grateful to some of my colleagues for aid and assistance in the laboratory when more than two hands were required.

SCHOOL OF PHARMACY

M.S. Examination Report - Pharmaceutics

Directions: At the conclusion of the examination for the M.S., the examining committee members should complete this document and the major professor should see that it is deposited in the student's permanent School of Pharmacy record.

Name of Candidate: DHUPAR, Kailash C.

Written M.S. Exam: Date _____ Score _____

Result: Pass (unrestricted) _____

Pass (Terminal M.S.) _____

Fail _____

Oral M.S. Exam: Date 12/16/75

Result: Pass (unrestricted) ✓

Pass (Terminal M.S.) _____

Fail _____

Signatures: 1. Jerry L. Carter (major professor)

2. George Zografi

3. Doyle D. Chambers

4. Peter Millard

Dissenting: _____

Comments (please initial): _____

DHUPAR, KAILASH CHANDRA
NAME

Candidate for Master of .....SCIENCE.....

PHARMACY
Major Department

Examined 12/17/75

Result PASSED

Reported to the Graduate Faculty

Degree granted: .....
Date

University of Wisconsin–Madison

To Professors:

CARSTENSEN, *Chairman*

ZOGRAFI

AMIDON

WELLING

You are hereby requested to act as a committee for the ~~written~~ oral examination of the candidate whose name is endorsed hereon.

By authority of the President of the University.

Robert M Bock

Dean

The Graduate School

Madison, 12/18 1975
(Date of Examination)

To the Graduate Faculty:
We, the undersigned, report that as a committee we have examined

Kailash Chandra Dhupar

whose major field is Pharmacy (Pharmaceutics)

We recommend that the candidate be admitted to the degree of Master of SCIENCE

In partial fulfillment of the requirements of the Master's degree the candidate offers a thesis entitled: (If no thesis has been required, kindly indicate the fact.)

Dissolution Rate Equations in Column Confined Dissolution.

Jun T. Carstensen
George Zografi
Isaac Abrahamson
Peter Lindenbaum

We report that the candidate has failed to pass a satisfactory examination and is not recommended for admission to the Master's degree.

TABLE OF CONTENTS

INTRODUCTION

There have been a large number of publications in the field of dissolution testing in recent years. Pernarowski (1) in a survey in 1973 showed one hundred different methods which had been published in literature. LeHir (2) also has described the technology in depth. It would seem that one disadvantage of such a profusion of methods would be that results from one method would not be comparable with results of another. It would, obviously, be advantageous if a means existed that would allow transformation of a result from one method to that of another for the purpose of comparison.

An even more serious problem is that of reproducibility of a method. If a dissolution rate test is performed in 'identical' equipment in different laboratories then results should hopefully be comparable. However, literature reports differently (3); differences in 'identical' pieces of apparatus may stem from such factors as (a) differences in vibration (4), (b) difference in abrasion (5), (c) differences in zero time (6) and (d) differences (of small magnitude) of dimensions or positional geometery (e.g. the point at which a rotating basket is positioned in the dissolution vessel (7)). Point (b) has been a well known fact to many investigators in the field of disintegration & dissolution. Metal screens are rough when initially purchased

(manufactured); this gives rise to abrasion of the dosage form (both in U.S.P. disintegration and dissolution rate apparatuses). However, continued exposure to 0.1N HCl will de-burr the wire mesh and make it smooth and reduce the abrasion, hence increase dissolution and disintegration times. The study reported here attempts to develop a means (not a dissolution rate method) for overcoming the stated poblems and to characterise a substance (oxalic acid) in such a fashion that it could be used as an internal standard.

THEORY

The fact that different methods give different results is due to variation in hydrodynamics from method to method. In essence the intrinsic dissolution rate constant is given by the Nernst-Brunner equation (8,9):

$$-dm/dt = Q(dC/dt) = k \cdot \Psi \cdot (S-C) \qquad \text{(Eq.1)}$$

where m is mass undissolved, t is time, Q is volume of dissolving liquid, C is concentration, Ψ is surface area of the powder at time t, and S is the saturation concentration. k is the intrinsic dissolution rate constant and is given by (10):

$$k = \frac{D\delta}{D+h\delta} \qquad \text{(Eq.2)}$$

where h is the thickness of a (supposedly stagnant) film of liquid adhered to the solid particles, D is the diffusion coefficient of the solute in the dissolving liquid, and δ is the dissolution rate constant at high agitation intensity. At high agitation intensities the liquid film will tend toward zero, hence $D >> h\delta$ and $\lim_{V\to\infty} k = \delta$. It is seen, that h is a function of liquid velocity, v (cm./sec), i.e.,

$$h = \phi(v,a) \qquad \text{(Eq.3)}$$

but as expressed in Eq.3 (and reported by Niebergall et al. (11)) h is also a function of the dimension (a cm.) of the dissolving particle. At low liquid velocity, the film thickness, h, is large, so that $h\delta >> D$ and Eq.2 becomes:

$$k = D/h = D/\phi(v,a) = \lambda(v,a) \qquad \text{(Eq.4)}$$

It is exactly the dependence on velocity that makes different methods give different results and also, partly, is responsible for different pieces of equipment of the same construction at times giving poor reproducibility.

Assuming the vessel used to be cylindrical makes it possible to describe a point in space in the vessel by use of cylindrical coordinates, i.e., by an angle, θ, a distance from center, r, and a height above the bottom, H. It is obvious that the liquid velocity, v, is a function of the position in the agitated vessel and also a function of time, i.e., at a particular point:

$$v = v(r,\theta,H,t) \qquad \text{(Eq.5)}$$

The average velocity $\bar{v}$ in the entire vessel at time t is given by:

$$\bar{v}(t) = \frac{1}{Q}\int_0^{2\pi}\int_0^{R}\int_0^{H_o} v(r,\theta,H,t)\,dH\cdot dr\cdot d\theta \qquad \text{(Eq.6)}$$

where Q is the volume of the dissolving liquid, R is the radius of the vessel and H_o is the height of liquid in the vessel. The average velocity for the duration (of time t') of the dissolution experiment is then:

$$\bar{v} = \frac{1}{t'} \int_0^{t'} \bar{v}(t)\, dt \qquad \text{(Eq.7)}$$

If one, hence, could determine the functions in Eq.5, one could describe a dissolution method either by the function or by its average value (Eq.7). However, such a determination is (usually) not possible, and furthermore the average velocity would (due to upper limit) still be a function of the t_{90} (t') of the particular test.

It is apparent, however, if for a standard substance the function in Eq.4, i.e., $k = \lambda(v,a)$ were known, then a particular dissolution method can be performed with a monodisperse sample of the standard substance with dimension a_o. The determined rate constant would be $k_{expt.} = \lambda(v,a_o)$ so that the average velocity could be expressed as :

$$\bar{v} = \lambda^{-1}(a_o, k_{expt.}) \qquad \text{(Eq.8)}$$

λ^{-1} is here the inverse function of (not the reciprocal value) λ .

If a relationship such as Eq.4 were established

then[a] differences between 'identical' pieces of apparatus could obviously be resolved, and, indeed, the standard substance could be used as an internal standard.

It should be pointed out that the film theory (8,9) has been subject to some criticism lately (12,13) in that the convective diffusion terms are neglected. However, these objections are primarily directed at the dissolution from a planar surface (as for example, in a Wood's apparatus (14)); where convective diffusion causes removal at the edges parallel to the flow; such a situation does not exist in a dissolving particle where there is rotational motion in the adsorbed film, so that the convective diffusion does not cause mass transport into the bulk solution. The general validity of the Nernst-Brunner theory in particular dissolution is evidenced by the agreement found by Carstensen and Patel (15) in dissolution of polydisperse powders with theoretical model based on the film theory. King (41) has

---

[a]There has been no attempt here to make a complete bibliography; only articles directly relevant to the particular argument in this study have been cited in the references. For a bibliography of methodology the reader is referred to reference 1.

reported that it is not necessary for the Nernst-Brunner Theory that the so called 'stagnant layer' be stagnant on the solid surface. The Nernst-Brunner layer may be a hydrodynamic boundary, which, rather than being stagnant represents a velocity field, with zero velocity at the solid boundary;this however is not incompatible with the concept that concentration is a function of the distance from the solid surface only.

EXPERIMENTAL

The test substance used was oxalic acid dihydrate[c]. The oxalic acid was recrystallised and classified by sieving described as follows: 100 g. of oxalic acid was dissolved by heat (70°c) in 200 c.c. of water and air cooled overnight to get crystals. The crystals were then filtered off and air dried at room temperature. The dried crystals were segregated into mesh fractions by means of U.S.P. sieves using Cenco Sieve Shaker[d]. The useful fractions were stored in desiccators over saturated Sodium chloride solution with excess solid Sodium chloride (33% relative humidity); this was done to avoid vitrification (Carstensen & Patel (15)).Various mesh fractions used in these experiments were: -10/+20, -20/+40 & -40/+60.

The dissolution experiments were performed in a column such as shown in Fig. 1. A female ground joint (A_1) was fused[e] onto the top of a 50 c.c. burette. A male ground joint (A_2) was fused onto a sintered glass filter in a 1cm. internal diameter pyrex tube. A stopcock (c), pyrex tubing and a

[c]Oxalic acid dihydrate, 97%, Aldrich Chemical Company, Inc., Milwaukee, Wisconsin 53233.

[d]Cenco-Meinzer Sieve Shaker, Central Scientific Co., Division of Cenco Instruments Corporation, 2600 Kostner Ave., Chicago, Ill. 60623.

[e]All fusing was done by glass blowing using pyrex glass and a gas-oxygen flame.

Fig.1: Apparatus used for dissolution rate studies.

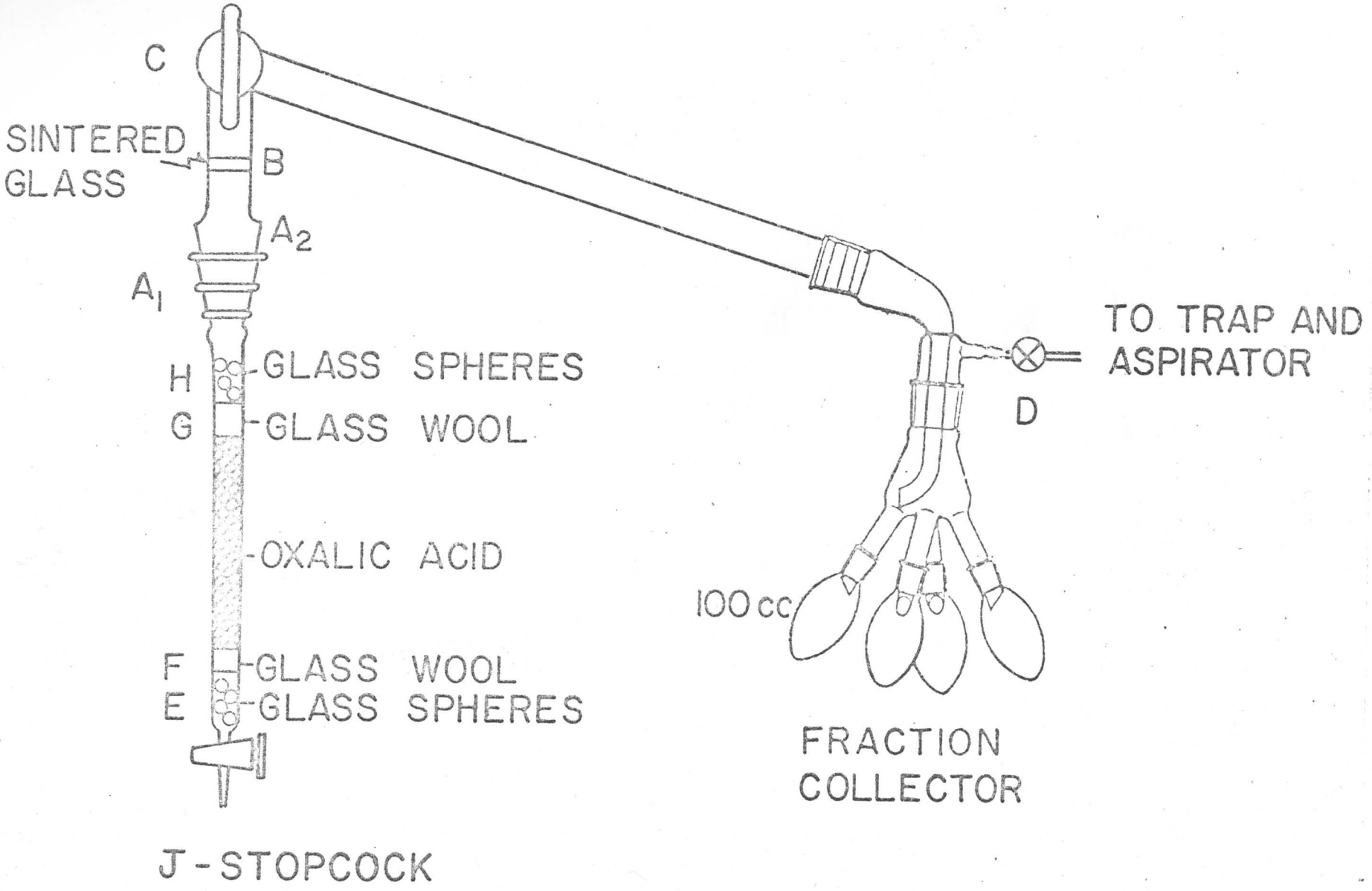
C
SINTERED GLASS
B
A2
A1
H
GLASS SPHERES
G
GLASS WOOL
OXALIC ACID
F
GLASS WOOL
E
GLASS SPHERES
J - STOPCOCK
TO TRAP AND ASPIRATOR
D
100 cc
FRACTION COLLECTOR

male joint were fused onto the other end of the sintered glass filter tube, and the tube bent beyond 'c' at the angle shown; the male joint fit the outlet joint of a commercial glass fraction collector[f] with four 100 c.c. collecting bulbs. The vacuum outlet of the fraction collector was connected to a manostat[g] to get same vacuum in all the experimental runs. The manostat was connected to an Erlenmeyer vacuum flask serving as a trap, and this in turn connected to a water aspirator via a stopcock, D. The tip of the burette stopcock, J, was attached via a piece of tygon tubing to a micrometric flow valve[h]. The rate of liquid flow could be governed by both this latter and the position of stopcock D.

The column was loaded with glass spheres at E to a depth of 1 cm., then with 1 cm. of glass wool (at F) and then with 40 cm. (ca. 33gm.) of oxalic acid dihydrate crystals of a given mesh sieve fraction. Glass wool (1cm.) and glass beads (8cm.) were then added at points G & H. The purpose of the glass beads at E is to rectify the turbulance which occurs

---

[f]Eck and Krebs Scientific Laboratory Glass Apparatus Inc. 27-09 40th. Ave.,Long Island City, N.Y.11101. Catalog No. 10525 and 10515.

[g]Manostat Corporation, 20 North Moore Street, N.Y.,N.Y.10013.

[h]Roger Gilmont Instruments Inc. 161 Great Neck Road,Great Neck, N.Y.11021. Micrometric capillary valve Cat.No. M7110.

at the pipe widening beyond the stopcock (J), (16). The purpose of the glass beads at H is to weight down the column so that it does not move upwards during experiments performed at high liquid velocity. The purpose of the sintered glass filter is to prevent passage of entrained small particles into the efflux beyond G. After the column had been packed, the burette stopcock was closed and C and D opened and the aspirator started to get a vacuum of 40 m.m. of Mercury. Just prior to the start of the experiment, C was closed and a 800 c.c. beaker with 0.1N HCl lifted up over the tip of the flow valve, and the burette stopcock and C then opened. Timers were started and the time required to fill each of the four collecting bulbs (t_i) recorded. The collector was turned by hand at the point when collection was changed from one bulb to the next. After noting the total length of the oxalic acid packed column, the length of the column[i] as a function of time was recorded during the experimental run at the point when one bulb was changed to the next. The amount of oxalic acid present in a fraction (m_i) was determined titrimetrically and the volume flow rate, V_i (c.c./sec.) and dissolution rate (dm_i/dt_i) were calculated. The feed used in the experiments were (a) 0.1N HCl and (b) 0.1N HCl containing varying concentrations of oxalic acid, viz.

---

[i]It takes two persons to collect results from one experiment..

degrees of saturation of 0.2, 0.3, 0.4, 0.6, & 0.8.

The specific surface area of a coarse solid as used here is small and cannot be determined by gas adsorption or by permeametry. The geometric surface areas can be obtained by microscopy, since the crystals can be approximated by parallelopipeds (15) (Fig. 2) of length L, breadth αB and height B. N= 50 crystals of a -10/+20 mesh cut were weighed; their dimensions (L and αB) were determined microscopically. The volume is then (since the sample is fairly monodisperse) $\alpha\bar{L}(\bar{B})^2$. Comparing the theoretical weight, $N\alpha\bar{L}(\bar{B})^2 \cdot \rho$ (where ρ =1.653 g./c.c.) to the actual weight allows calculation of α, and hence the specific geometric surface area can be found to be $2\bar{L}(\alpha\bar{B}) + 2\bar{L}(\bar{B}) + 2\alpha(\bar{B})^2$. The same procedure was carried out for all the mesh fractions used in the study. The results are shown in table VI.

The surface area term of interest, as shall be seen at a later point, is A, the surface area present in one cm. length of column. It is of interest to see if or how 'A' changes as a function of position and time. For this purpose a column was packed alternately with glass wool and oxalic acid (10/20 mesh); the column, in this fashion, consisted of six sub-columns. A dissolution experiment was then carried out for 67 sec. and the length of various sections

Fig. 2: Actual and Idealised crystals of oxalic acid.

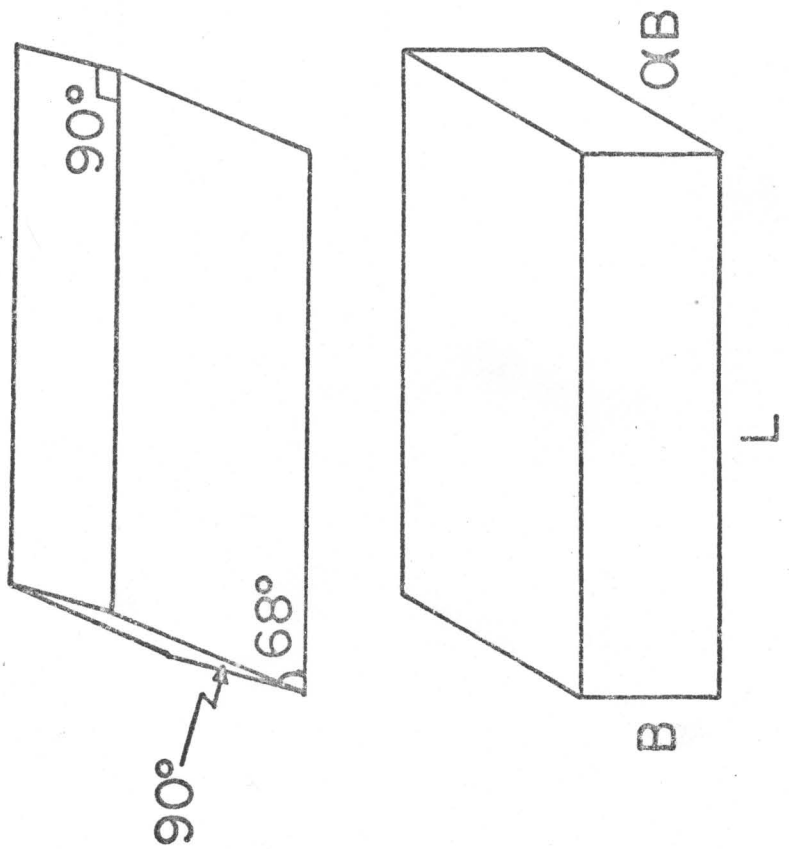
90°
68°
90°
αB
B
L

measured. The geometric surface area of each section was then determined microscopically and divided by the length to give the value of 'A'.

It was desired, at one point, to check the concentration profile along the column. For this purpose, a duplicate column was prepared, with four side arms, as shown in Fig.3. The side arms were short (1.5 cm.) and could accomodate a rubber plug, into which a hypodermic syringe was inserted. Prior to insertion of the plug, the space in front of it, as shown in the figure, was filled with glass wool. At a particular point in an experiment, the flow was stopped, and samples drawn from the four positions, and assayed for oxalic acid.

To be able to determine the activation energy of dissolution, dissolution experiments were carried out at 10°C, 15°C and 37°C in addition to those done at room temperature. The column that was used earlier, described on page 8, was jacketed from outside by a pyrex tubing of larger internal diameter and sealed. Two side arms were connected to the pyrex jacket for the circulation of water. The dissolution liquid, before passing through the column, was thermostated to a specific temperature in a jacketed beaker by circulating water controlled at the temp. of interest. The experiment was run and the samples were collected in the usual way.

Fig. 3: Apparatus used for studying the dependence of concentration (C) on distance (x).

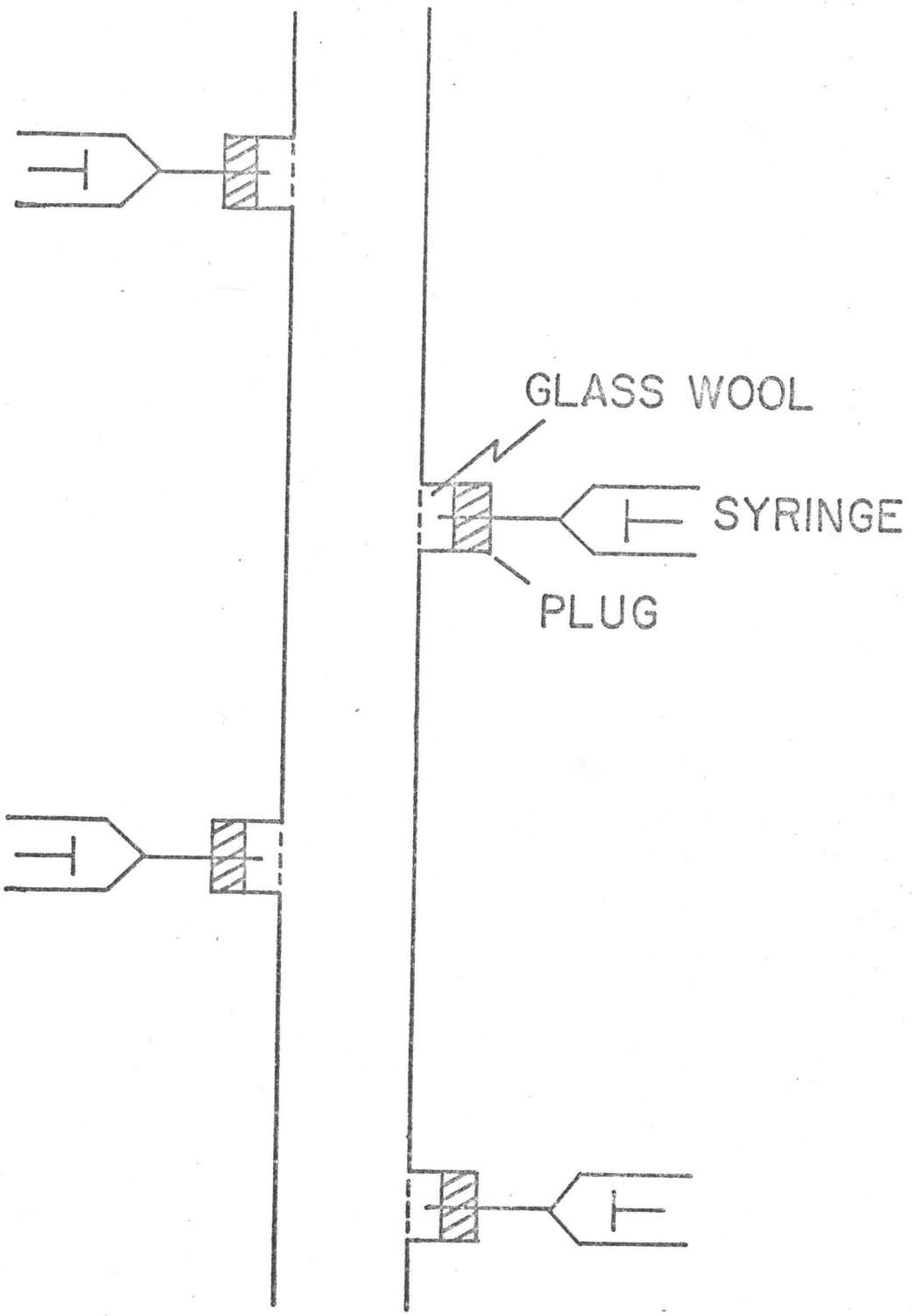
GLASS WOOL
SYRINGE
PLUG

The solubility of oxalic acid dihydrate in N/10 HCl was determined at various temperatures. The results are shown in Table V and Fig.18 . The determinations were made using a thermostated shaker bath[j].

---

[j]Aquatherm Water Bath Shaker, Model No. R-86, New Brunswick Scientific Co., Inc., New Brunswick, N.J.

RESULTS

The dissolution experiments were done using apparatus shown in Fig. 1. The variation of column length as a function of time were recorded (data for one of the experiments is shown in Table I) and found to be linear as shown in Fig.4 to Fig. 17 for various cases studied. The fractions collected in four bulbs, after dissolution, were quantitatively transferred to volumetric flasks and diluted to the mark with known volume of water using burette. The readings are shown in Table II. 10.0 ml. of the diluted fractions were titrated with standard sodium hydroxide solution using Phenolphthalein as an indicator. 10.0 ml. of the feed dissolution liquid (called 'blank') was also titrated to make possible calculation of the exact value of the degree of saturation of blank (f). The number of milliequivalents of sodium hydroxide (in gm.) required to titrate the collected fractions and the amounts of oxalic acid dissolved during dissolution were calculated (shown in Table III). The calculated dissolution rates, dm/dt (g./sec.), the flow rates, V (c.c./sec.) and the dissolution rate constants, k (cm./sec.) are given in Table IV.

The calculation of 'f' is shown as follows:

10.0 ml. of blank = 7.37 milliequivalents of NaOH.

10.0 ml. of N/10-HCl = 1.06 milliequivalents of NaOH.

Oxalic acid in 10.0 ml. of blank = 6.3 milliequivalents of sodium hydroxide.

Table I: Column heights and time intervals for dissolution of -10/+20 mesh size oxalic acid crystals.

	Column height (cm.)	Time interval (sec.)	Cumulative time (sec.)
	40.5	-	0.0
	38.4	45.6	45.6
1.	35.8	18.6	64.2
2.	33.0	20.2	84.4
3.	29.9	22.0	106.4
4.	26.9	24.0	130.4

Weight of oxalic acid crystals packed in column = 31.36 gm.

Temprature of feed liquid = 24°C.

Solubility of oxalic acid crystals in N/10 HCl solution = 0.152 g./ml.

Degree of saturation of feed liquid = 0.26.

Fig.4: Column length as a function of time plot.

⓪ : f = 0.0, V = 2.48 c.c./sec., 25°C.

⊙ : f = 0.0, V = 3.61 c.c./sec., 25°C.

⊖ : f = 0.0, V = 1.64 c.c./sec., 25°C.

Particles are -10/+20 mesh.

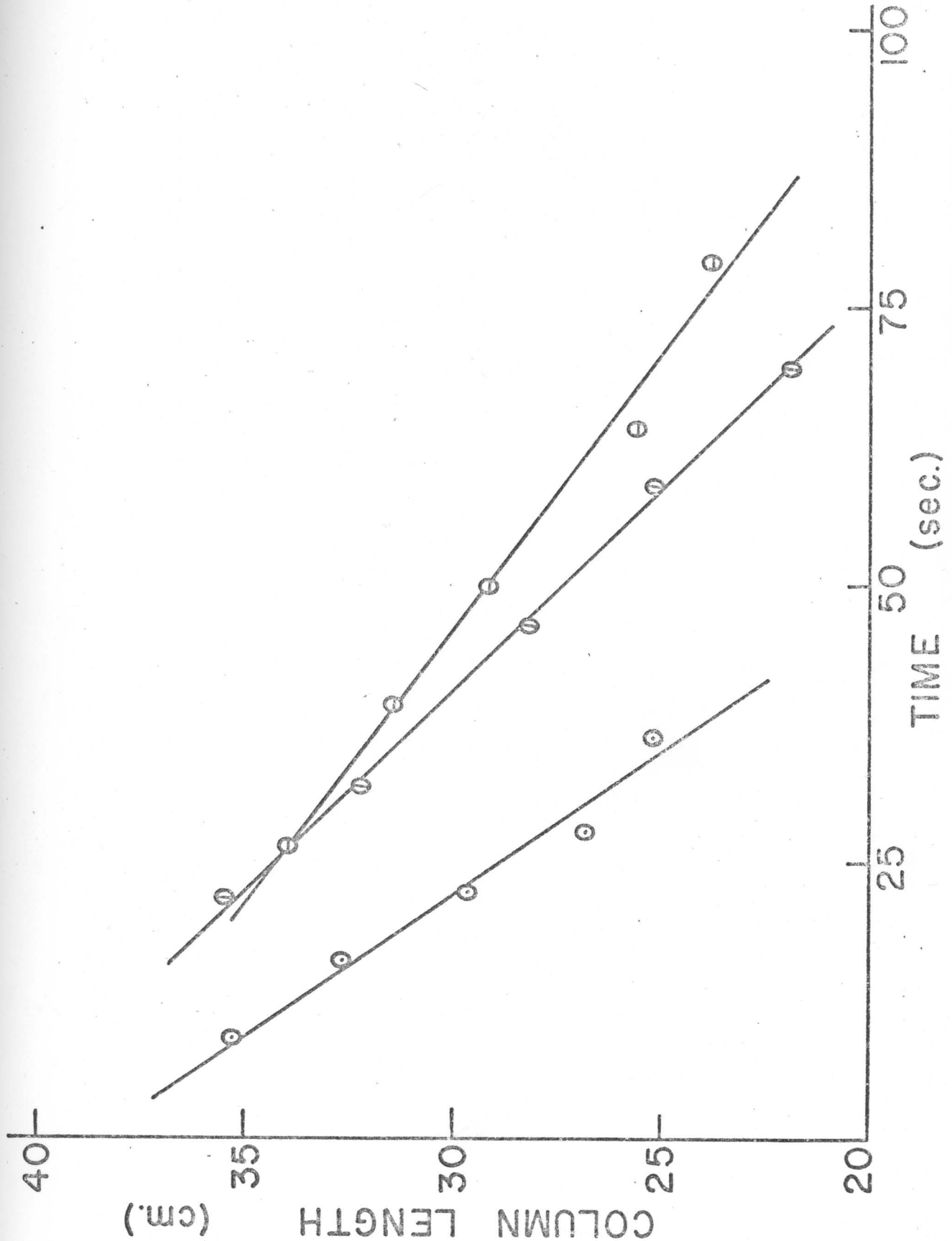
COLUMN LENGTH (cm.)
40
35
30
25
20
TIME (sec.)
25
50
75
100

Fig.5: Column length as a function of time plot.

⊖ : f = 0.26, V = 1.02 c.c./sec., 24°C.

⊙ : f = 0.27, V = 5.47 c.c./sec., 23°C.

◍ : f = 0.27, V = 3.20 c.c./sec., 23°C.

Particles are -10/+20 mesh.

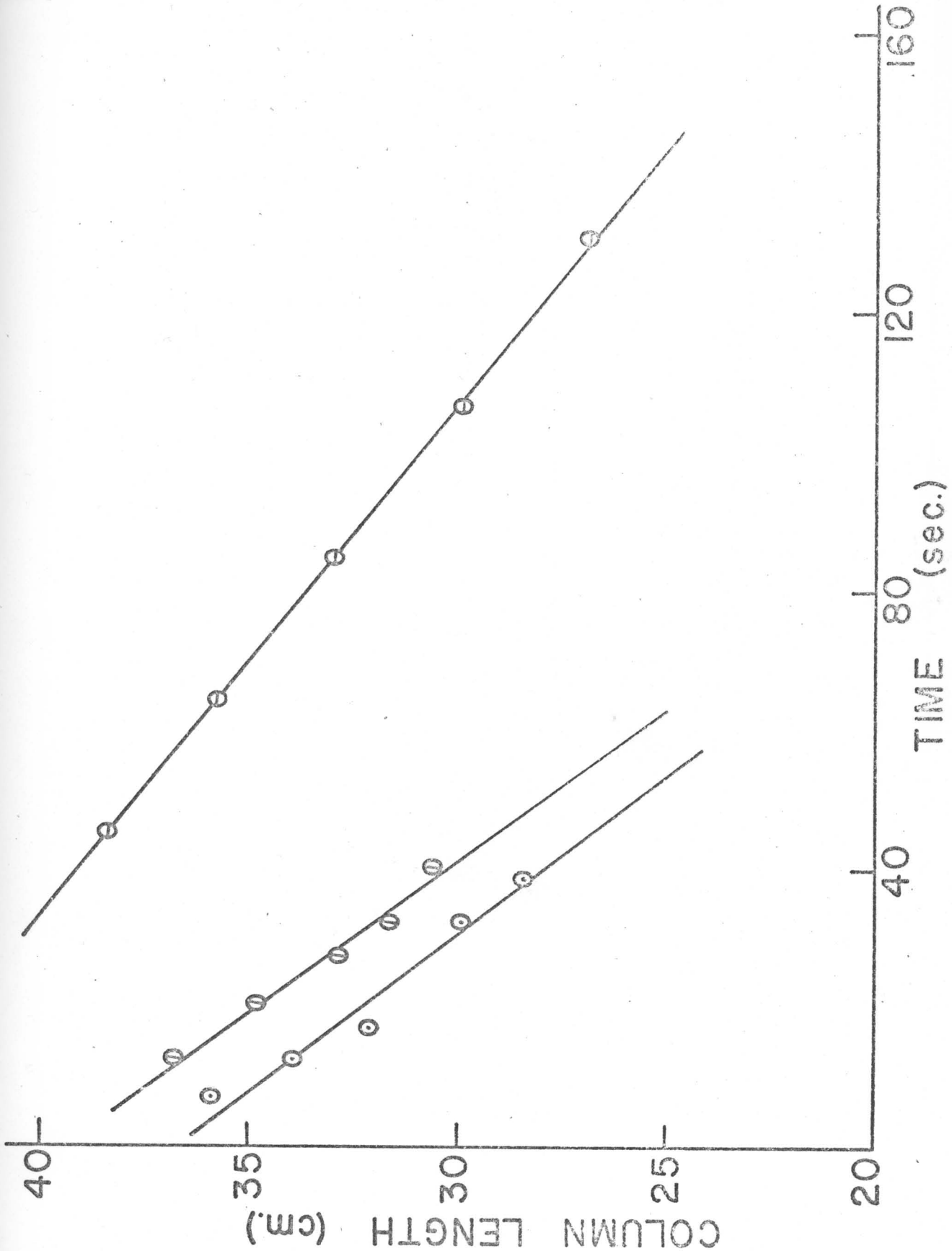
COLUMN LENGTH (cm.)
40
35
30
25
20
TIME (sec.)
40
80
120
160

Fig.6: Column length as a function of time plot.

⊙ : f = 0.62, V = 4.50 c.c./sec., 21°C.

⊖ : f = 0.60, V = 1.62 c.c./sec., 22°C.

◐ : f = 0.60, V = 2.45 c.c./sec., 22°C.

Particles are -10/+20 mesh.

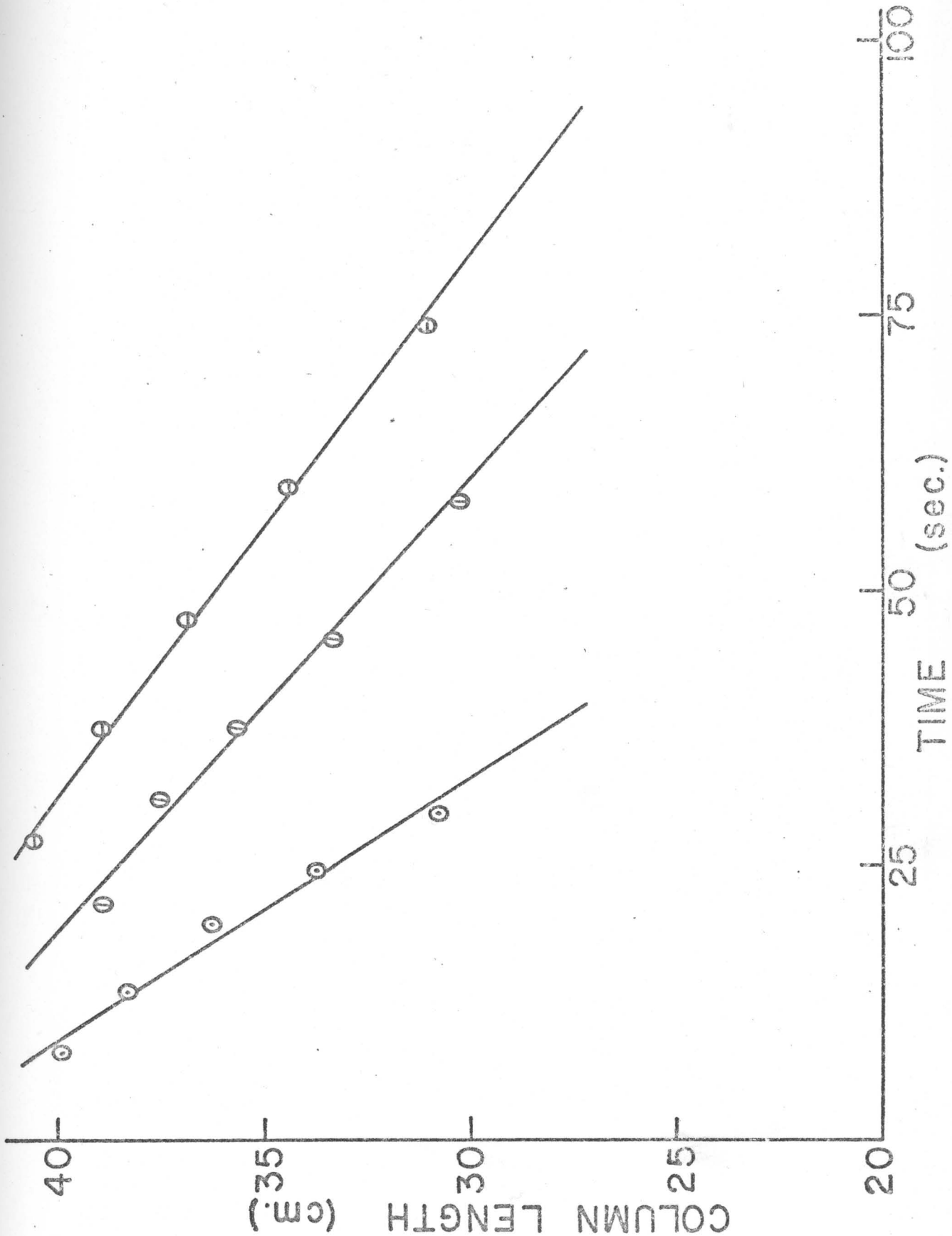
COLUMN LENGTH (cm.)
40
35
30
25
20
25
50
75
100
TIME (sec.)

Fig.7: Column length as a function of time plot.

⊙ : f= 0.0, V= 3.42 c.c./sec., 24°C.

⊖ : f= 0.0, V= 0.90 c.c./sec., 23°C.

◐ : f=0.0, V= 1.30 c.c./sec., 24°C.

Particles are -20/+40 mesh.

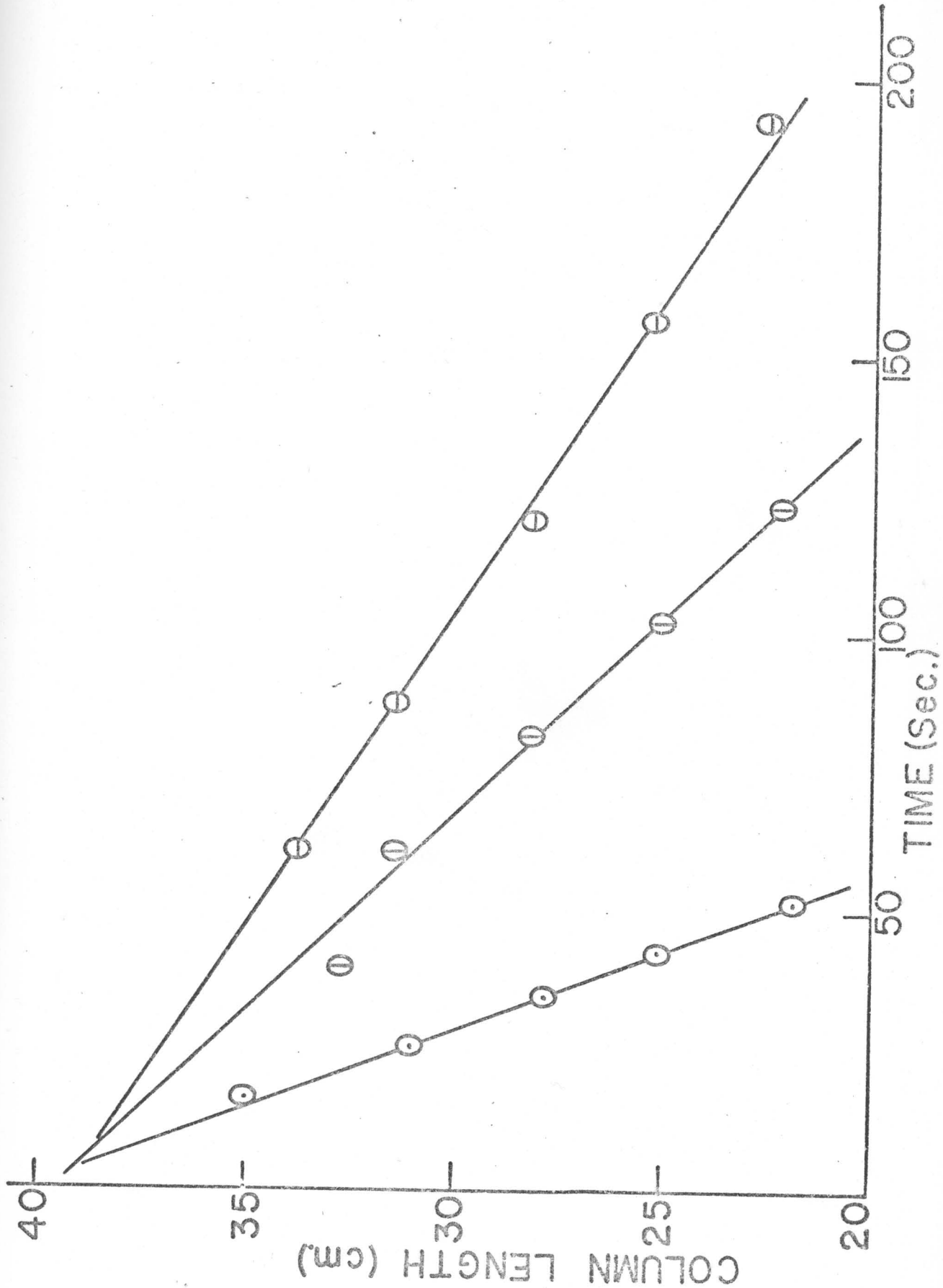
COLUMN LENGTH (cm.)
40
35
30
25
20
50
100
150
200
TIME (Sec.)

Fig.8: Column length as a function of time plot.

⓪ : f= 0.19, V= 2.56 c.c./sec., 21°C.

⊙ : f= 0.18, V= 3.27 c.c./sec., 21°C.

⊖ : f= 0.18, V= 2.03 c.c./sec., 21°C.

Particles are -20/+40 mesh.

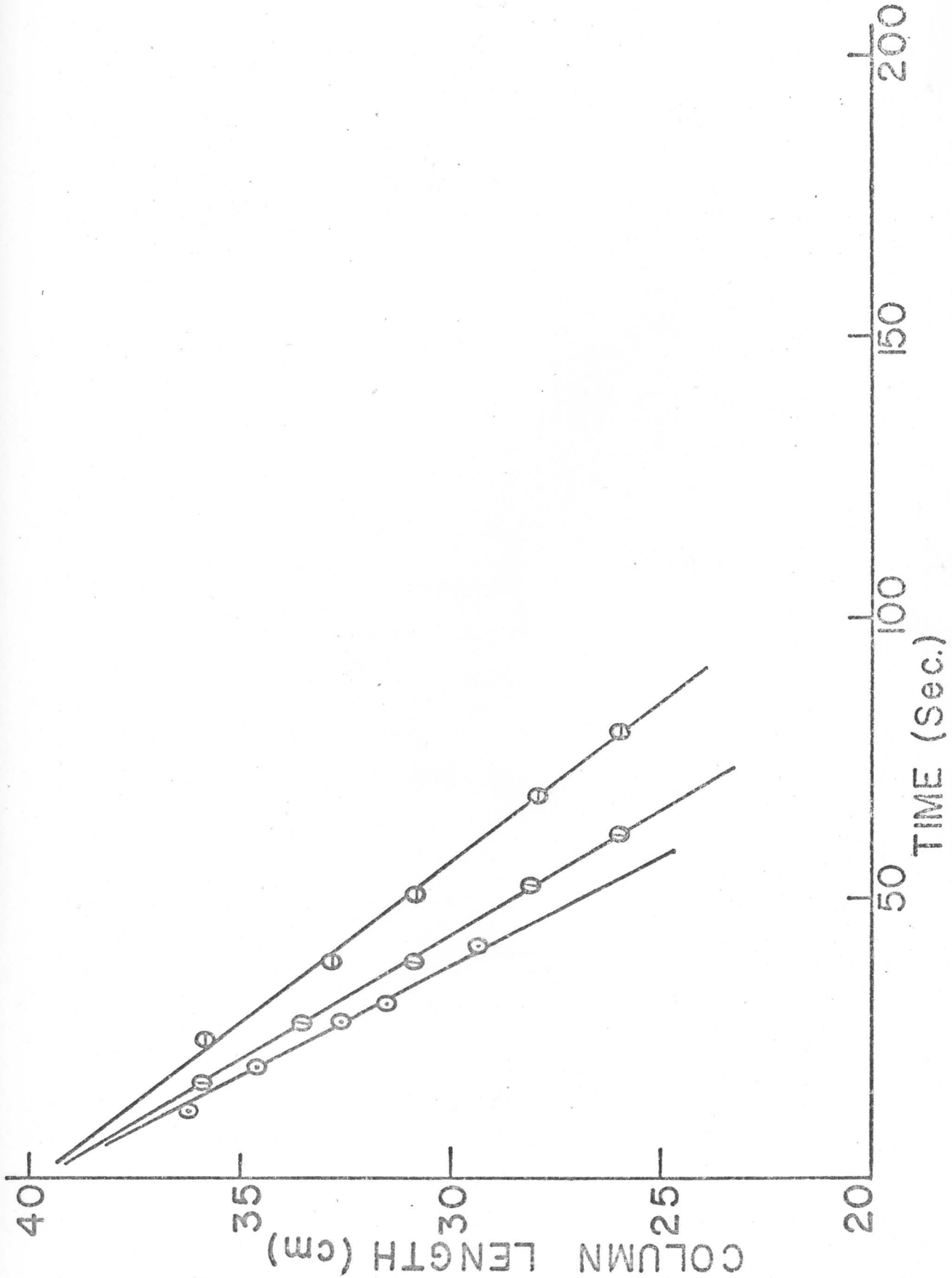
COLUMN LENGTH (cm)
40
35
30
25
20
50
100
150
200
TIME (Sec.)

Fig.9: Column length as a function of time plot.

⊙: f= 0.35, V= 4.17 c.c./sec., 22°C.

⊖: f= 0.34, V= 0.75 c.c./sec., 22°C.

⓪: f= 0.36, V= 2.13 c.c./sec., 21°C.

Particles are -20/+40 mesh.

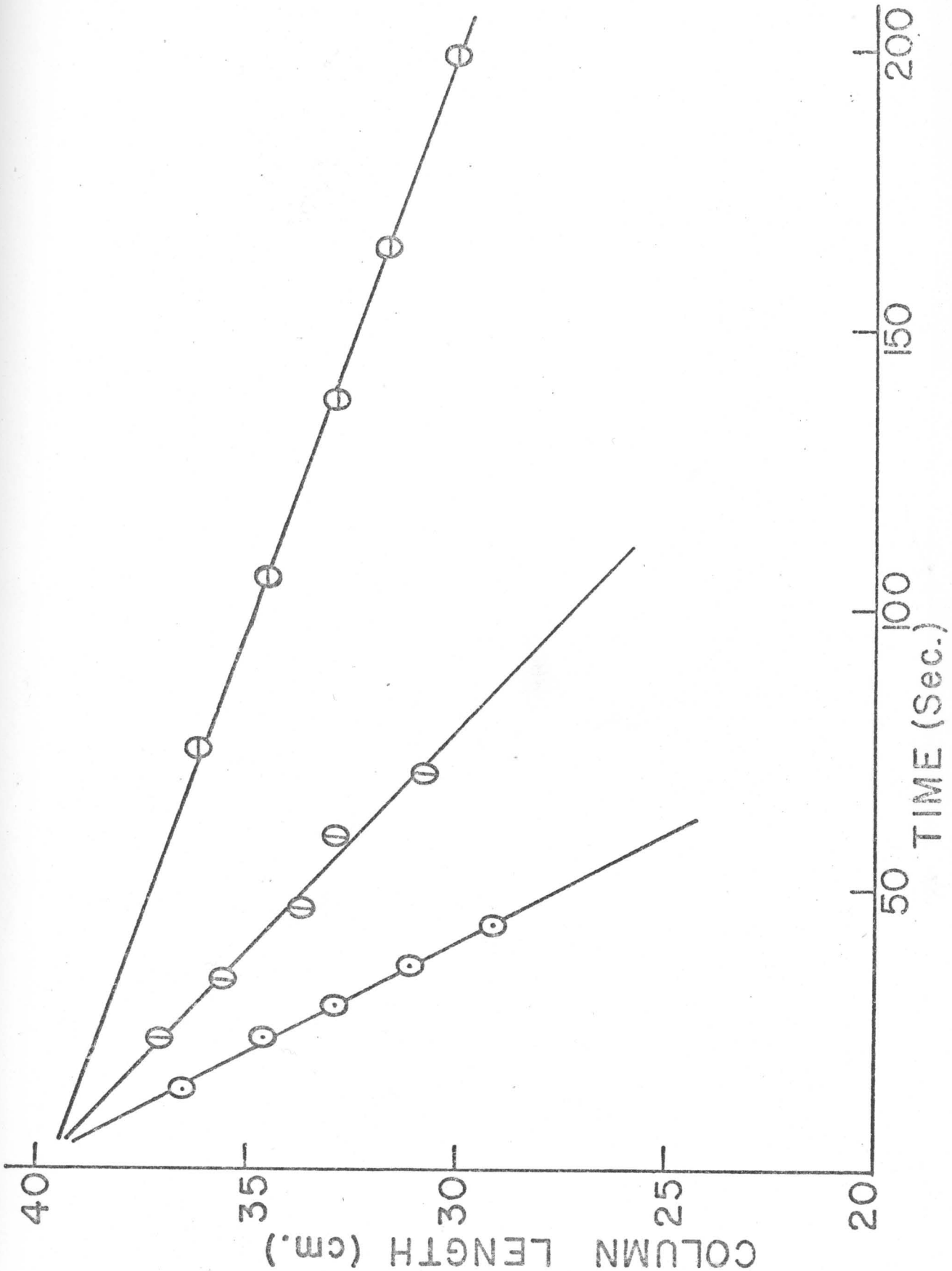
COLUMN LENGTH (cm.)
40
35
30
25
20
50
100
150
200
TIME (Sec.)

Fig.10: Column length as a function of time plot.

⊙ : f= 0.52, V= 2.53 c.c./sec., 22°C.

⊖ : f= 0.52, V= 0.61 c.c./sec., 22°C.

◐ : f= 0.52, V= 2.24 c.c./sec., 22°C.

Particles are -20/+40 mesh.

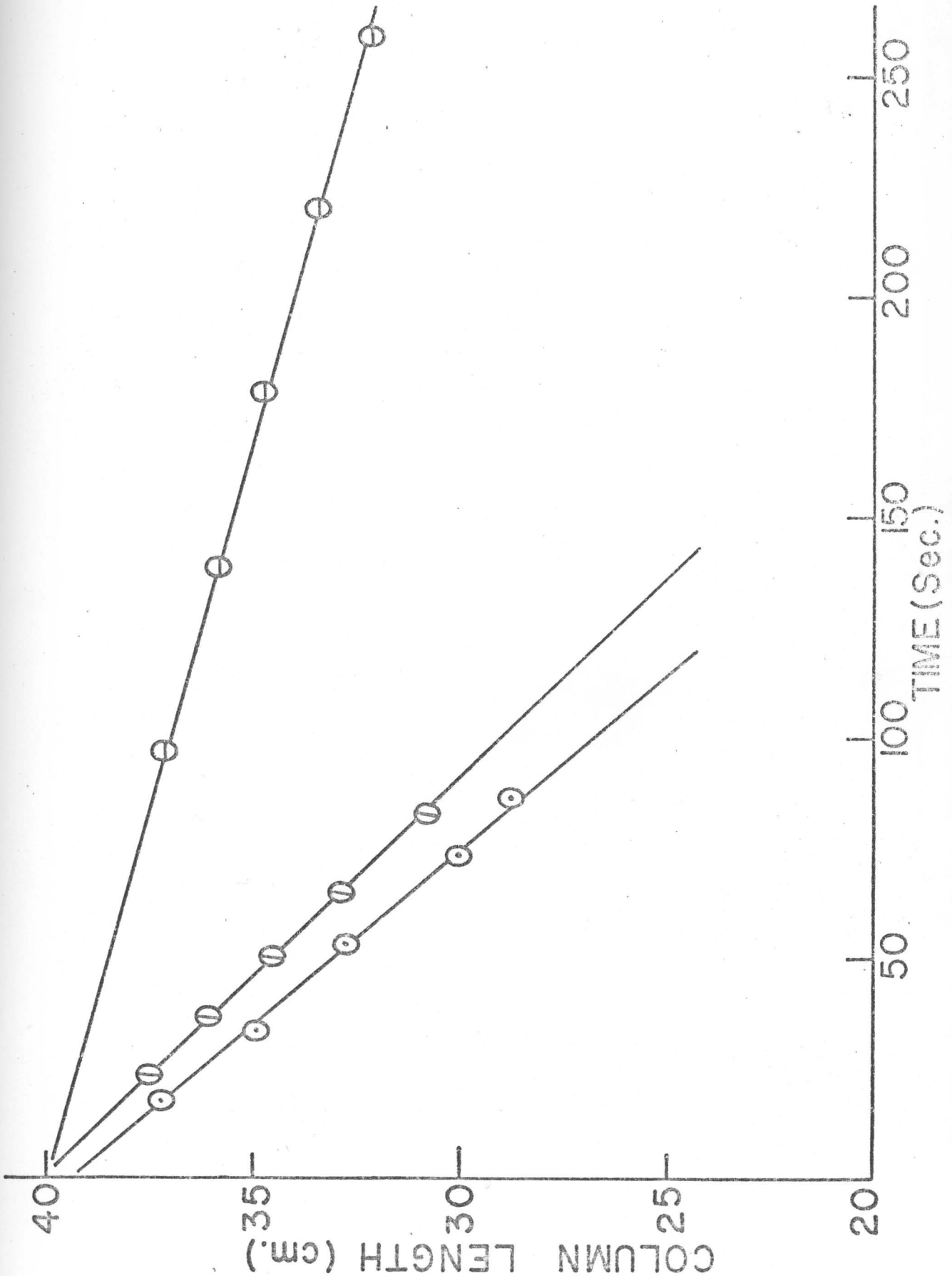
COLUMN LENGTH (cm.)
40
35
30
25
20
50
100
150
200
250
TIME (Sec.)

Fig.11:Column length as a function of time plot.

⊙ : f= 0.67 , V= 2.35 c.c./sec., 23°C.

⊖ : f= 0,68 , V= 1.37 c.c./sec., 23°C.

◍ : f= 0.70 , V= 2.13 c.c./sec., 22°C.

Particles are -20/+40 mesh.

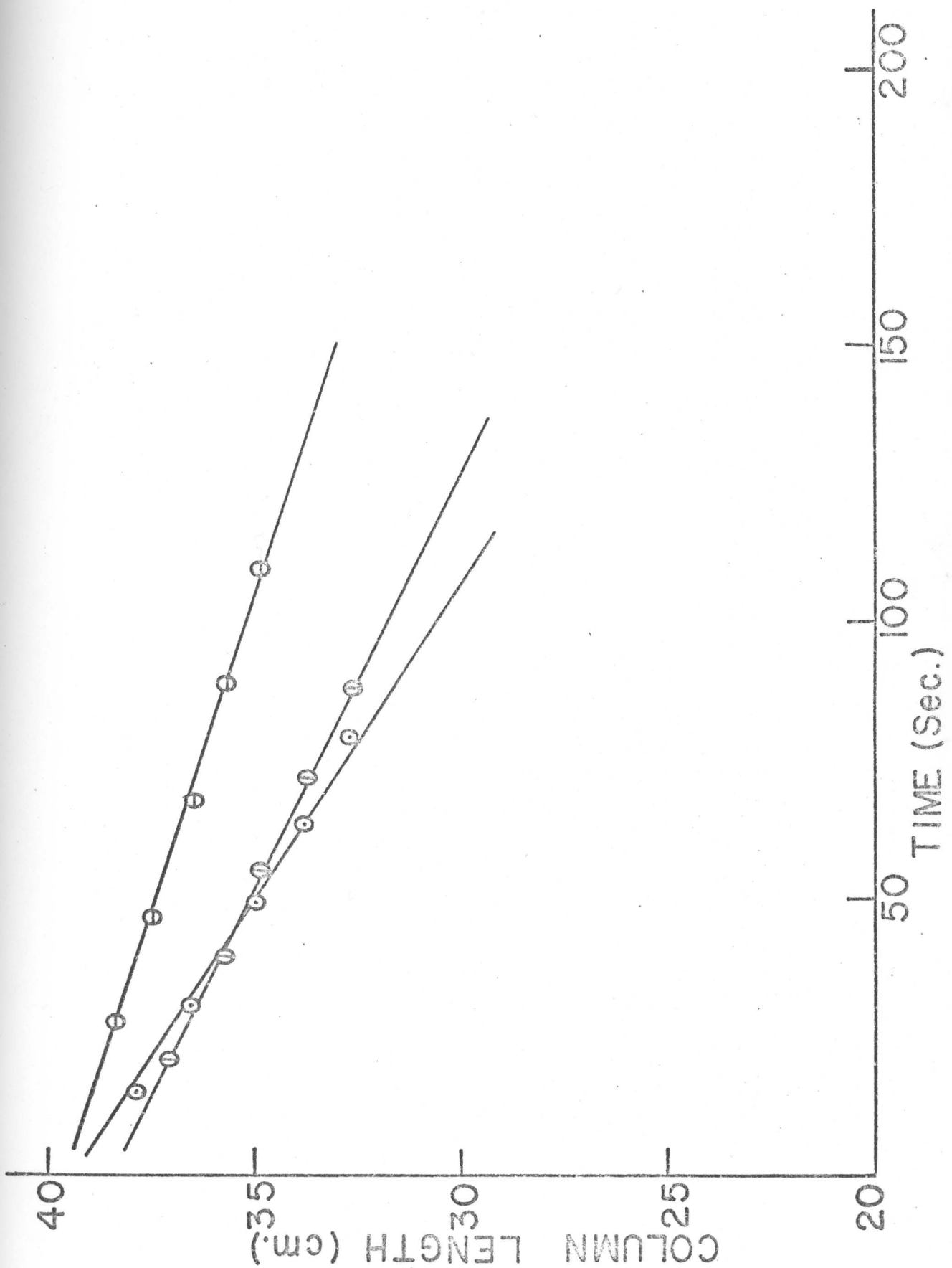
COLUMN LENGTH (cm.)
40
35
30
25
20
TIME (Sec.)
50
100
150
200

Fig.12: Column length as a function of time plot.

⊙ : f = 0.0, V = 1.41 c.c./sec., 22°C.

◐ : f = 0.0, V = 1.30 c.c./sec., 21°C.

⊖ : f = 0.0, V = 1.57 c.c./sec., 22°C.

Particles are -40/+60 mesh.

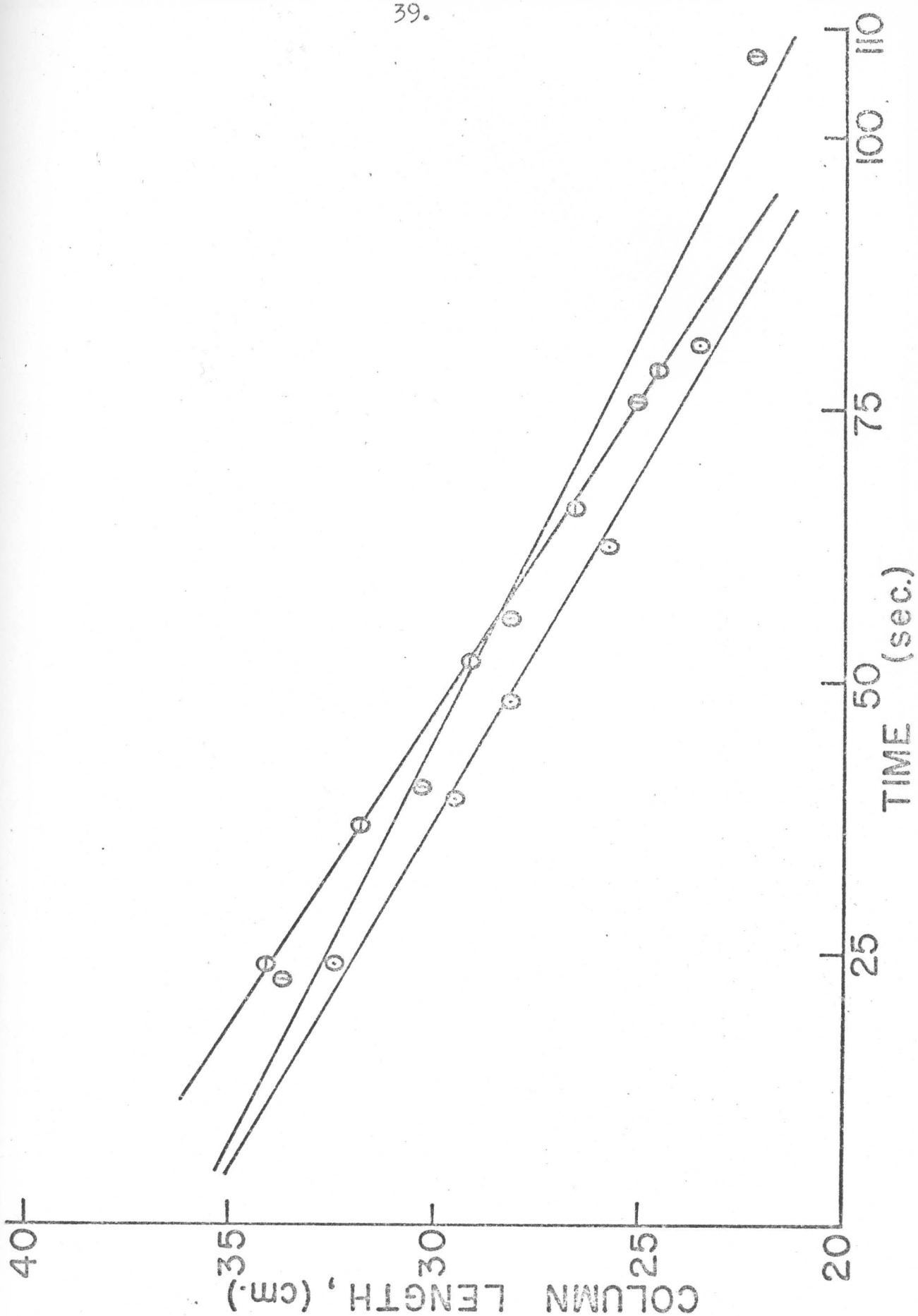
COLUMN LENGTH, (cm.)
40
35
30
25
20
TIME (sec.)
25
50
75
100
110

Fig.13: Column length as a function of time plot.

⓪ : f = 0.29, V = 1.16 c.c./sec., 23°C.

⊙ : f = 0.29, V = 1.45 c.c./sec., 23°C.

⊖ : f = 0.32, V = 1.02 c.c./sec., 21°C.

Particles are -40/+60 mesh.

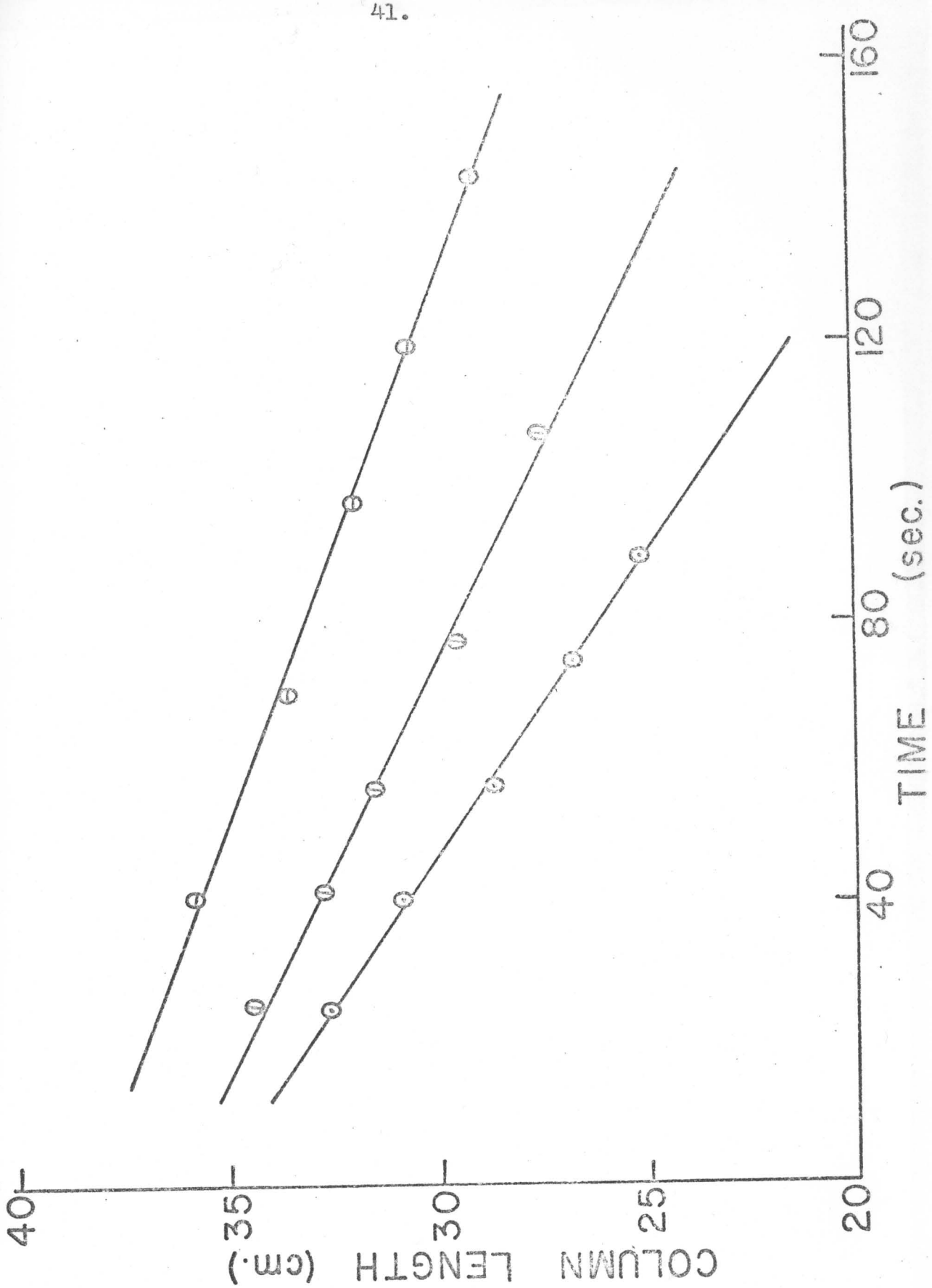
COLUMN LENGTH (cm.)
40
35
30
25
20
TIME (sec.)
40
80
120
160

Fig.14: Column length as a function of time plot.

⊙ : f = 0.59, V = 1.17 c.c./sec., 21°C.

◐ : f = 0.60, V = 1.06 c.c./sec., 22°C.

⊖ : f = 0.58, V = 0.85 c.c./sec., 23°C.

Particles are -40/+60 mesh.

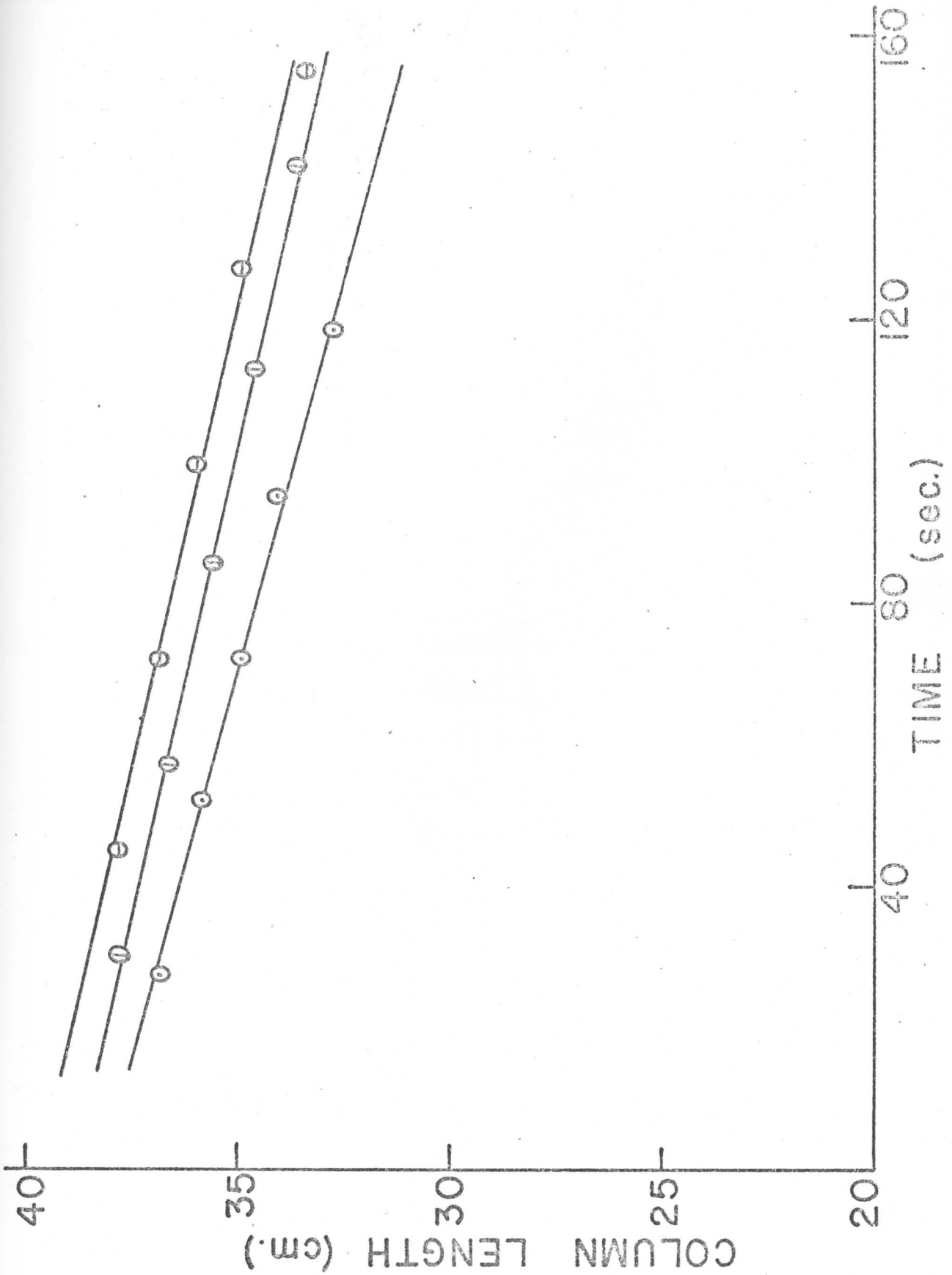
COLUMN LENGTH (cm.)
40
35
30
25
20
TIME (sec.)
40
80
120
160

Fig. 15. Column length as a function of time plot.

⓪ : f = 0.0, V = 2.08 c.c./sec.

⊖ : f = 0.0, V = 2.16 c.c./sec.

Particles are -10/+20 mesh.

Temperature of the incoming liquid = 10°C.

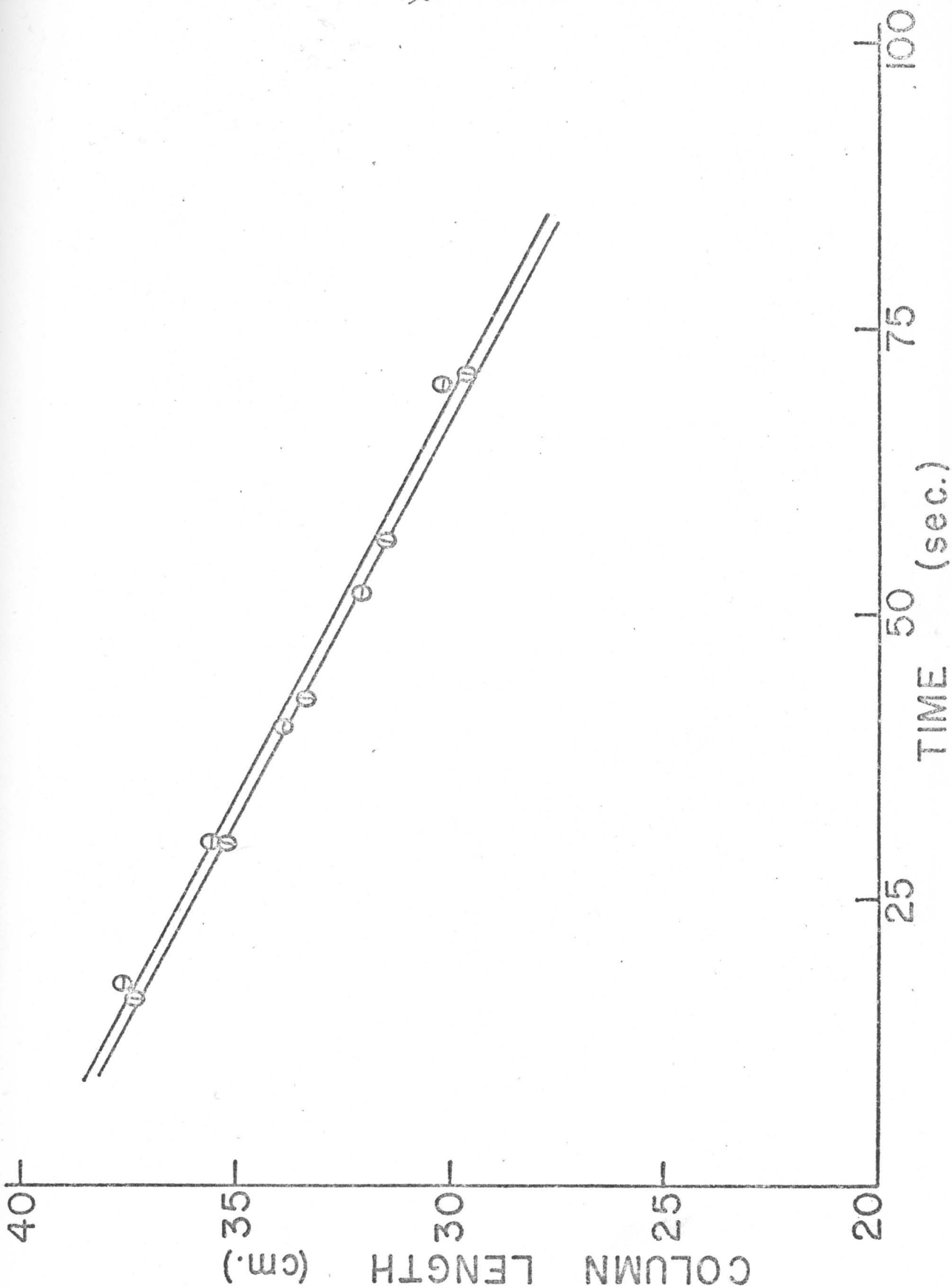
COLUMN LENGTH (cm.)
40
35
30
25
20
25
50
75
100
TIME (sec.)

Fig. 16. Column length as a function of time plot.

⓪ : f = 0.0, V = 2.36 c.c./sec.

Θ : f = 0.0, V = 1.90 c.c./sec.

Particles are -10/+20 mesh.

Temperature of the incoming liquid = 15°C.

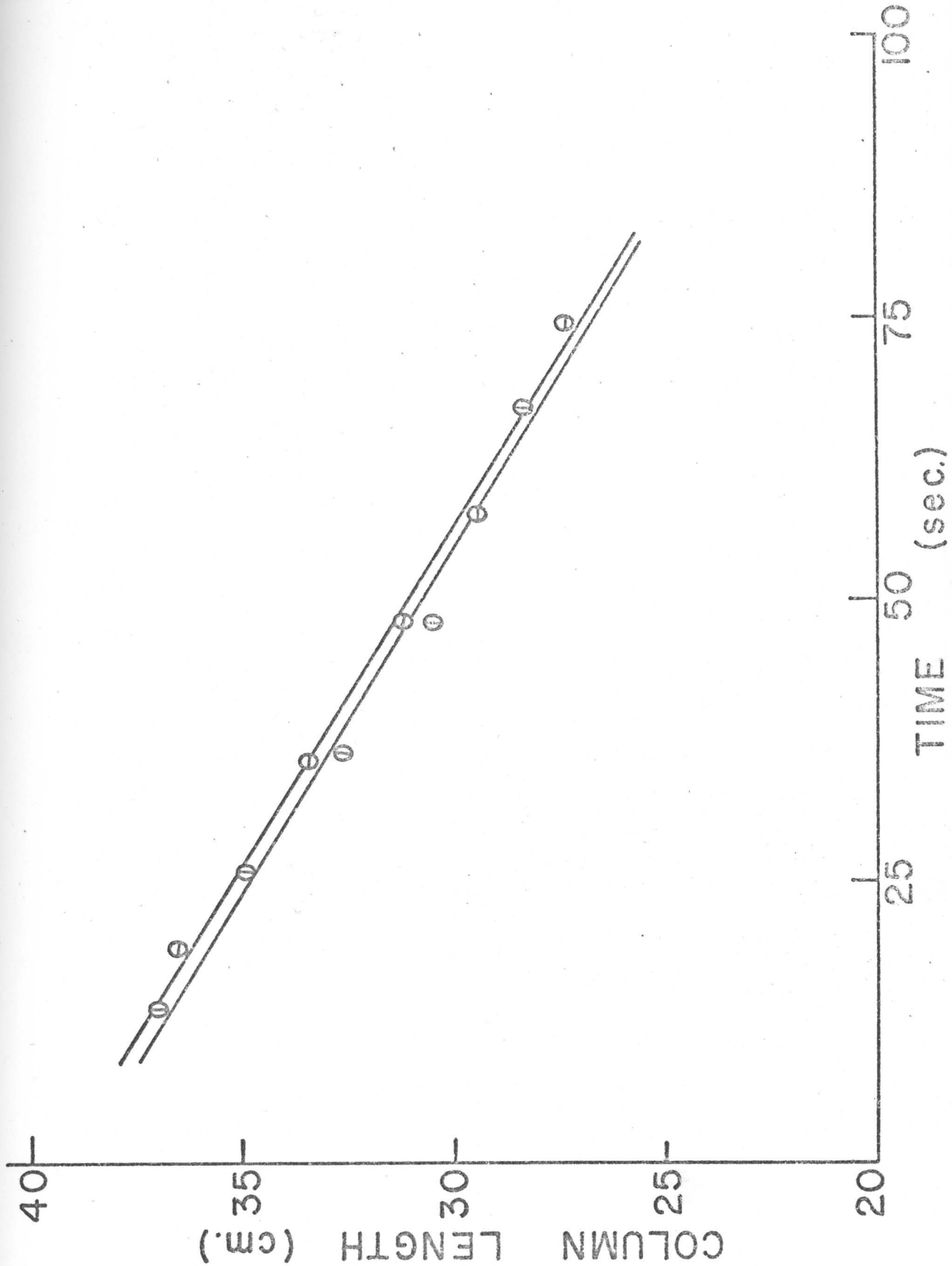
COLUMN LENGTH (cm.)
40
35
30
25
20
TIME (sec.)
25
50
75
100

Fig. 17. Column length as a function of time plot.

⊕ : f = 0.39, V = 2.89 c.c./sec.

⊖ : f = 0.39, V = 2.27 c.c./sec.

Particles are -10/+20 mesh.

Temperature of incoming liquid = 37°C.

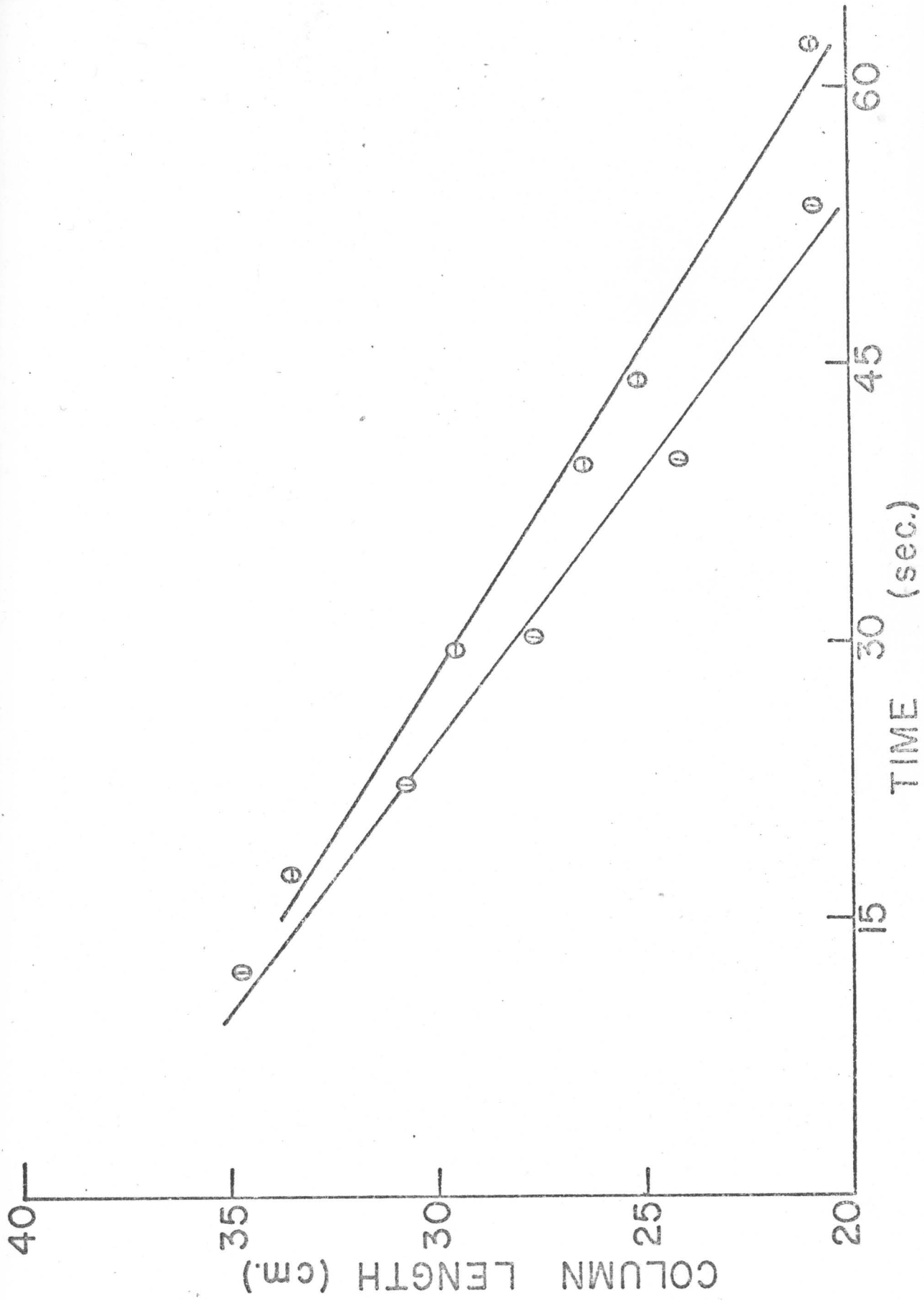
COLUMN LENGTH (cm.)
40
35
30
25
20
TIME (sec.)
15
30
45
60

Table II: Volume of dissolution fractions collected.

	Volume of water used (ml.)	Diluted to (ml.)	Volume of fractions collected. (ml.)
1.	32.60	50.0	17.40
2.	28.95	50.0	21.05
3.	28.20	50.0	21.80
4.	23.25	50.0	26.75

Table III: Amounts of oxalic acid dissolved from column.

Number of milliequivalents of sodium-hydroxide for titration of fractions.	Number of milliequivalents of sodium-hydroxide for feed liquid.	Number of milliequivalents of sodium hydroxide for oxalic acid dissolved from column.	Weight of oxalic acid dissolved from column.
Blank = 7.37	-	-	0.46 g.
1. 34.39	12.82	21.57	1.36 g.
2. 38.70	15.51	23.19	1.46 g.
3. 39.32	16.07	23.25	1.47 g.
4. 48.68	19.72	28.96	1.83 g.

Table IV: Dissolution rates, flow rates and dissolution rate constants.

	Dissolution rates dm/dt (gm./sec.)	Flow rates V (c.c./sec.)	Dissolution rate constants $k \times 10^4$ (cm./sec.)
1.	0.073	0.94	9.35
2.	0.072	1.04	9.44
3.	0.067	0.99	9.32
4.	0.076	1.11	10.91

Table V: Temperature dependent solubility of oxalic acid in N/10 Hydrochloric acid solution.

	Temperature ($t^oC.$)	Absolute temperature (T^oK)	1000/T ($^oK^{-1}$)	Solubility 'S' (g./ml.)	ln S + 3
1.	20	293.15	3.41	0.132	0.975
2.	25	298.15	3.35	0.156	1.142
3.	30	303.15	3.30	0.175	1.257
4.	35	308.15	3.25	0.210	1.439

Least squares fit: $\ln S = -\frac{2839}{T} + 7.65$

10.0 ml. of blank contains 0.40 gm. of oxalic acid.

$$f = \frac{\text{Amount of oxalic acid in blank (g./ml.)}}{\text{Solubility of oxalic acid in N/HCl (g./ml.)}}$$

N/10 HCl

$$= \frac{0.04}{0.152} = 0.26.$$

The calculation of 'q' (the degree of saturation of efflux (outgoing) liquid) is as follows:

Oxalic acid dissolved from the column in the first fraction collected $= \frac{1.36}{17.4} = 0.078$ g./ml.

Total amount of oxalic acid in the efflux liquid = weight of oxalic acid in the blank + weight of oxalic acid dissolved from the column = 0.04 + 0.078 = 0.118 g./ml.

$$q = \frac{\text{Amount of oxalic acid in the efflux liquid (g./ml.)}}{\text{Solubility of oxalic acid in N/10-HCl (g./ml.)}}$$

$$= \frac{0.118}{0.152} = 0.78.$$

Calculation of A_o :

A_o (Surface area of oxalic acid crystals per unit length of column) = (Specific surface area of oxalic acid crystals x amount of oxalic acid packed in column) / (Total length of the column).

$$A_o = \frac{40 \cdot 31.36}{40.5} = 30.97 \text{ cm.}^2/\text{cm.}$$

The solubility of oxalic acid in N/10 hydrochloric acid solution was determined at different temperatures and the results are shown in Table V and plotted in Fig. 18.

The calculation of 'α' and the specific surface areas of various mesh fractions found microscopically are indicated in Table VI. Finally rate constants were calculated according to equation number 22 (described later) for all the conditions used.

Fig.18: Temperature dependence of Solubility of Oxalic acid in N/10 Hydrochloric acid solution.

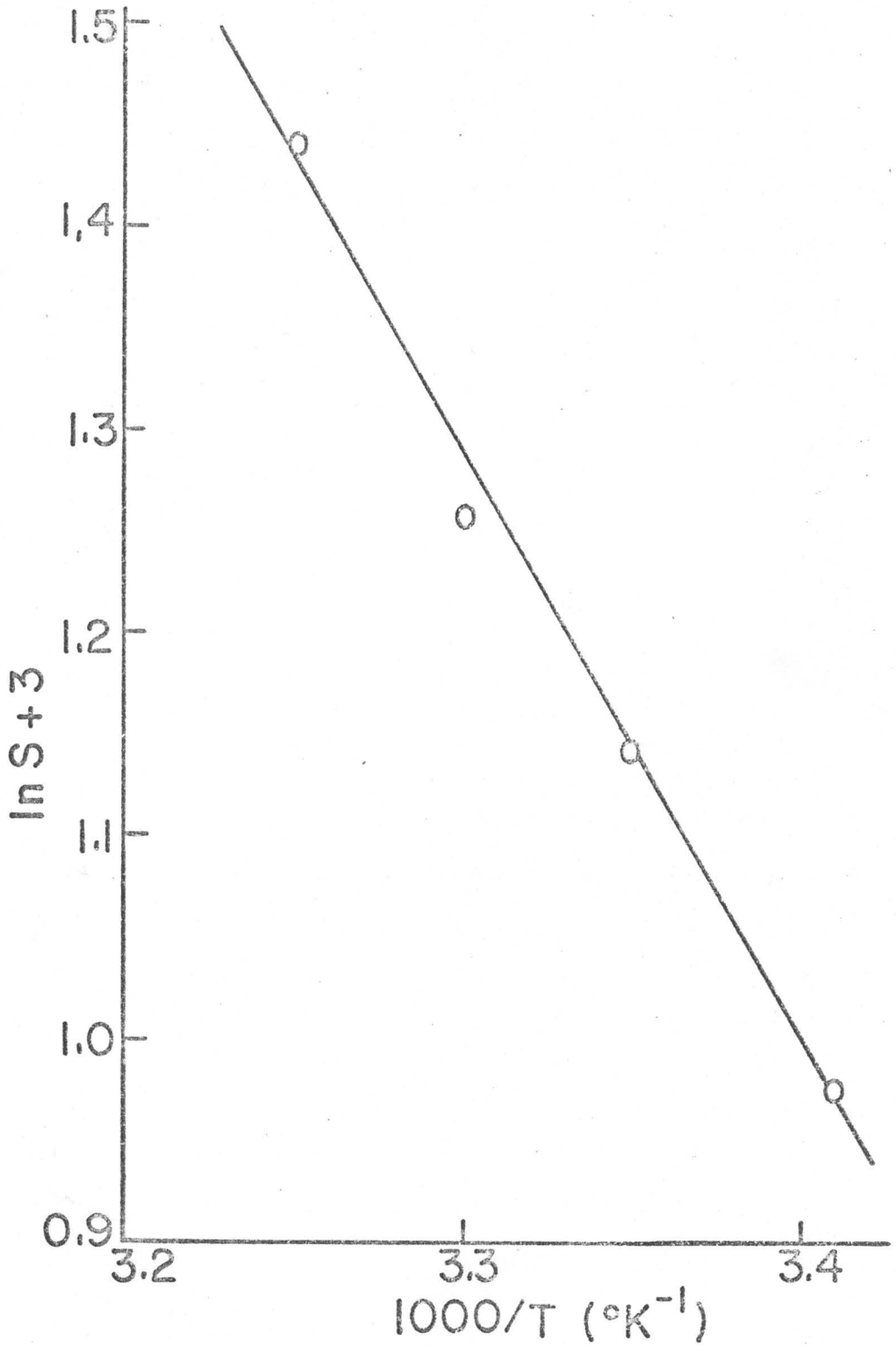
1.5
1.4
1.3
1.2
1.1
1.0
0.9
ln S+3
3.2
3.3
3.4
1000/T (°K⁻¹)

Table VI: Microscopic measurements of oxalic acid crystals and the calculation of α.

Mesh size	Number of crystals measured (N)	Average length $\overline{L}$ (μ)	Average breadth $\alpha\overline{B}$ (μ)	Calculated weight (g.) $\overline{L}\cdot\overline{B}^2\cdot\alpha\cdot N\cdot\rho$	Actual weight (g.)	Ratio = α = Calculated wt. / Actual wt.
-10/+20	50	3972	1370	0.62	0.22	2.81
-20/+40	50	1965	529	0.045	0.022	2.05
-40/+60	80	1210	316	0.016	0.0077	2.08
-60/+80	100	400	144	0.0014	0.0010	1.40

Average α = 2.1

Specific surface areas: ($cm.^2/gm.$)

-10/+20 mesh	40
-20/+40 mesh	84
-40/+60 mesh	127
-60/+80 mesh	190

Density of oxalic acid crystals = 1.653 g./c.c. (ρ)

'μ' stands for microns.

DISCUSSION

Consider a column of solid powder of length ℓ cm. and cross-section Ω cm.^{2} as shown in Fig.19. The surface area (cm.^{2}) of the amount of powder (b gm.) in one cm. length of column is denoted A (cm.^{2}/cm.). The liquid enters from the bottom of the column at a rate of V_i cm.^{3}/sec. It will dissolve solid from the column and exit with a rate of V' cm.^{3}/sec., where V' includes the volume increase due to the dissolved solid. If V denotes the average of V_i and V', then, if ε is the porosity of the powder, the linear velocity ($\bar{v}$ cm./sec.) will be given by (17):

$$\bar{v} = V/(\Omega \cdot \varepsilon) \qquad \text{(Eq.9)}$$

Let one cm. length of column having Ω cm.^{3} of volume contain b gm. of powder of density ρ g./c.c., then porosity ε is given by:

$$\varepsilon = 1 - \frac{b}{\Omega \cdot \rho} \qquad \text{(Eq.10)}$$

It was observed in this study, that under the conditions imposed the liquid was always fairly close to saturation upon exit. If one denotes this concentration qS, where q, the degree of saturation, is close to unity, then following

Fig.19: Nomenclature used: A_x surface area per cm. of column length, x distance from top of column, ℓ length of column at time t, S saturation concentration, f degree of saturation of feed, q degree of saturation of effux and C_x concentration at point x in the column.

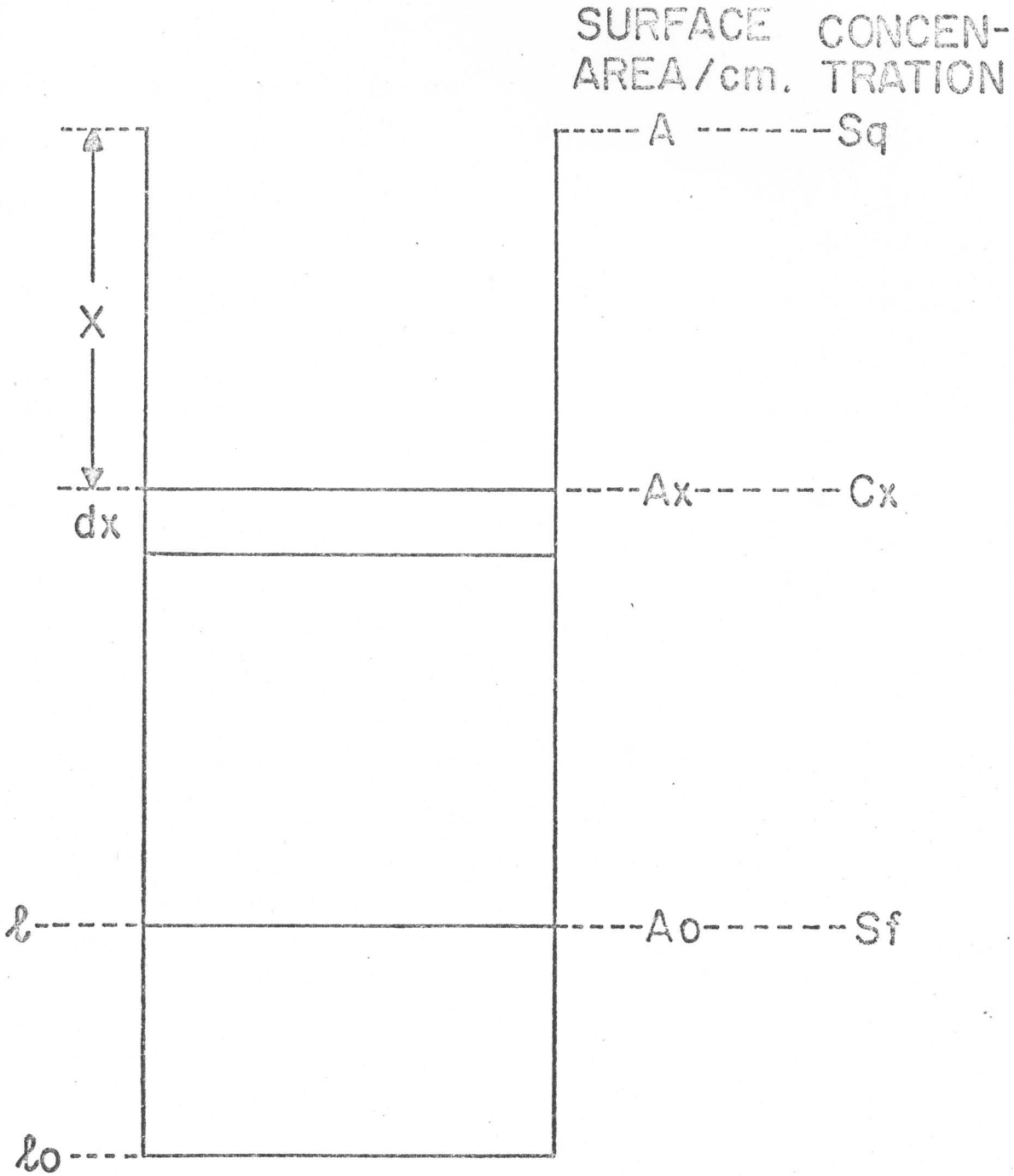
SURFACE AREA/cm.
CONCEN-TRATION
A
Sq
X
Ax
Cx
dx
ℓ
Ao
Sf
ℓo

will hold: in t seconds V·t c.c. will have passed through the column and have saturated to a degree of Sq, i.e., will have dissolved V·t·S·(q-f) g., if the incoming liquid is of a degree of saturation of'f'.Since there are b gm. of solid powder per linear column (cm.), V·t·S·(q-f)/b cm. will have disappeared, i.e.,

$$l = l_o - \frac{V \cdot S \cdot (q-f)}{b} \cdot t = l_o - \alpha t \qquad \text{(Eq.11)}$$

so that the column length should decrease linearly in time. That this is so is seen from Figs. 4 to 17. The slopes should be proportional to the liquid velocity (cm^3/ sec.). That this is so is seen in Figs.20 to 22, where slopes of the column length vs. time plots are plotted against the liquid velocities. The plots are linear and goes through the origin as dictated by:

$$\alpha = [S(q-f)/b] \cdot V = \beta \cdot V \qquad \text{(Eq.12)}$$

where: $$\beta = (S/b) \cdot (q-f) = -\frac{S}{b} f + \frac{S}{b} q \qquad \text{(Eq.13)}$$

Hence, if the slopes, β, from Fig.20-22 are plotted versus the degree of saturation, f, of the incoming liquid, a linear plot should result; these plots are shown in Figs. 23 & 24.

Fig. 20: Column decrease rate, α ($= \frac{d\ell}{dt}$), as a function of flow rate, V (c.c./sec.) of -10/+20 mesh particles.

⊖ : f = 0.0

⓪ : f = 0.61.

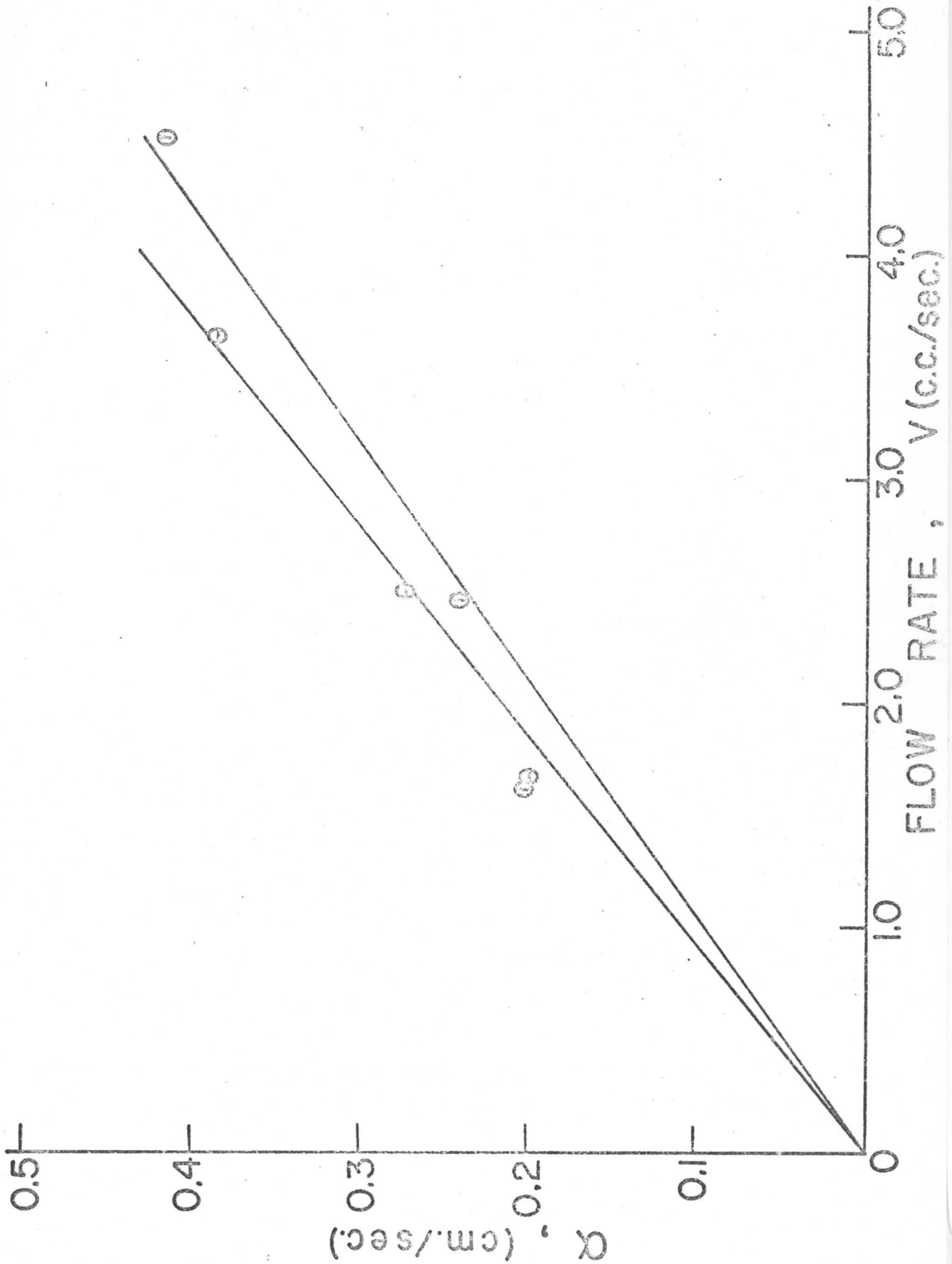
0.5
0.4
0.3
0.2
0.1
0
α , (cm./sec.)
1.0
2.0
3.0
4.0
5.0
FLOW RATE , V (c.c./sec.)
①
②
③
④
⑤

Fig.21: Column decrease rate, α, as a function of flow rate (V, c.c./sec.) of -20/+40 mesh particles.

○ : f = 0.0

◔ : f = 0.18

◑ : f = 0.35

◕ : f = 0.52

● : f = 0.68.

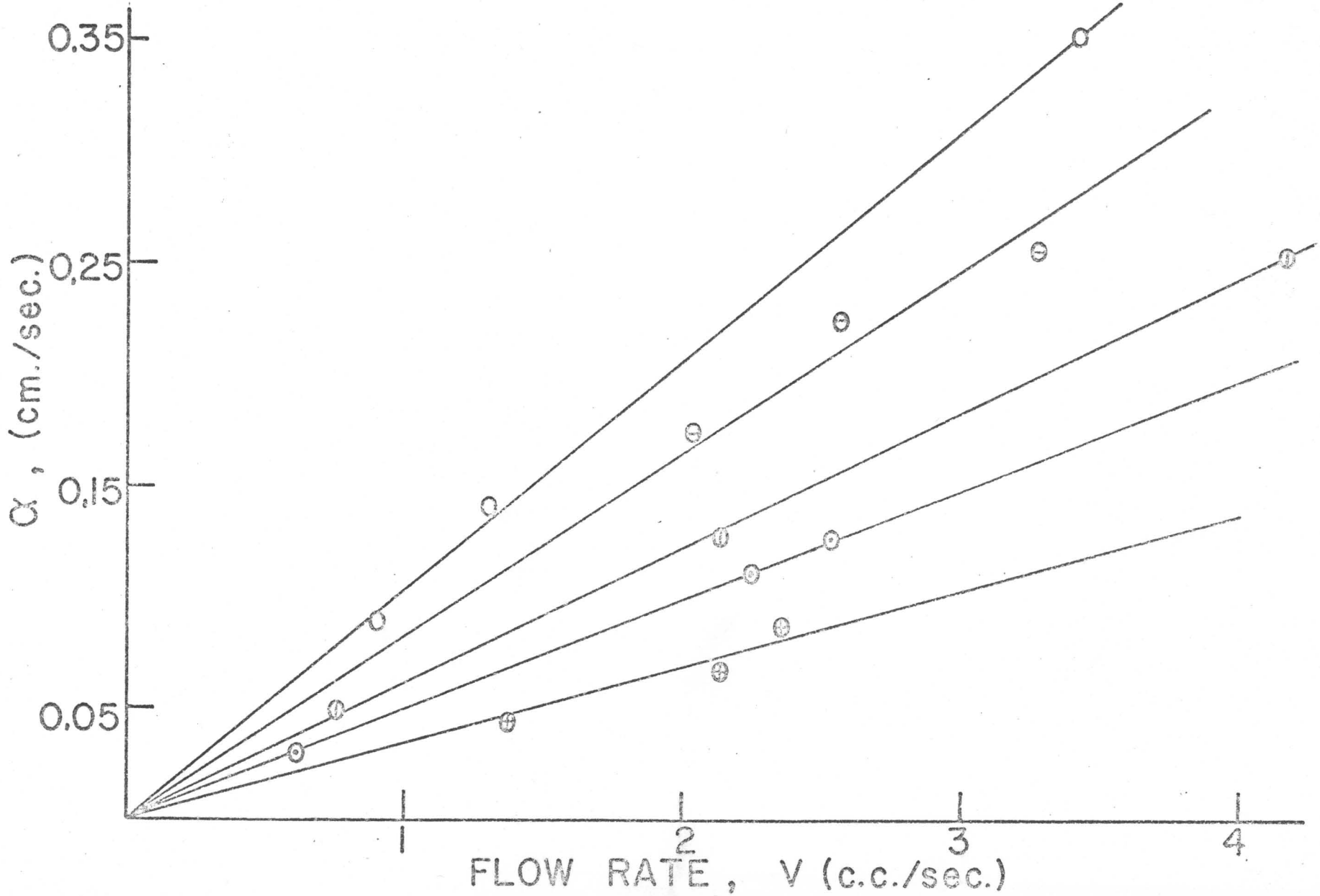
0.35
0.25
0.15
0.05
α , (cm./sec.)
1
2
3
4
FLOW RATE , V (c.c./sec.)

Fig.22: Column decrease rate, α (cm./sec.) , as a function of flow rate, V (c.c./sec.) of -40/+60 mesh particles.

⊖ : f = 0.0

◐ : f = 0.30

⊙ : f = 0.59.

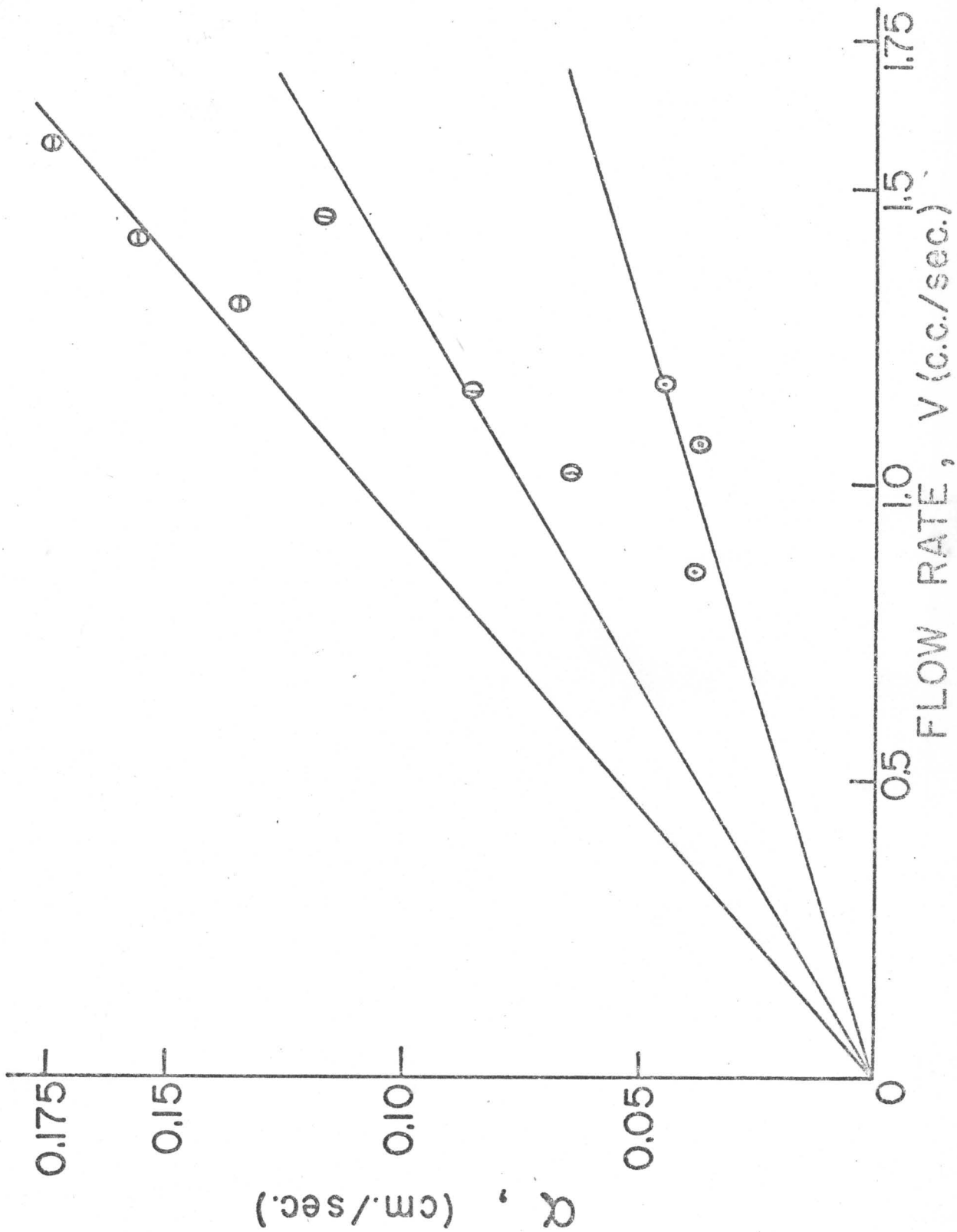
0.175
0.15
0.10
0.05
0
0.5
1.0
1.5
1.75
FLOW RATE, V (c.c./sec.)
α , (cm./sec.)

Fig.23: $d\alpha/dV = \beta$ as a function of 'f' for -20/+40 mesh particles.

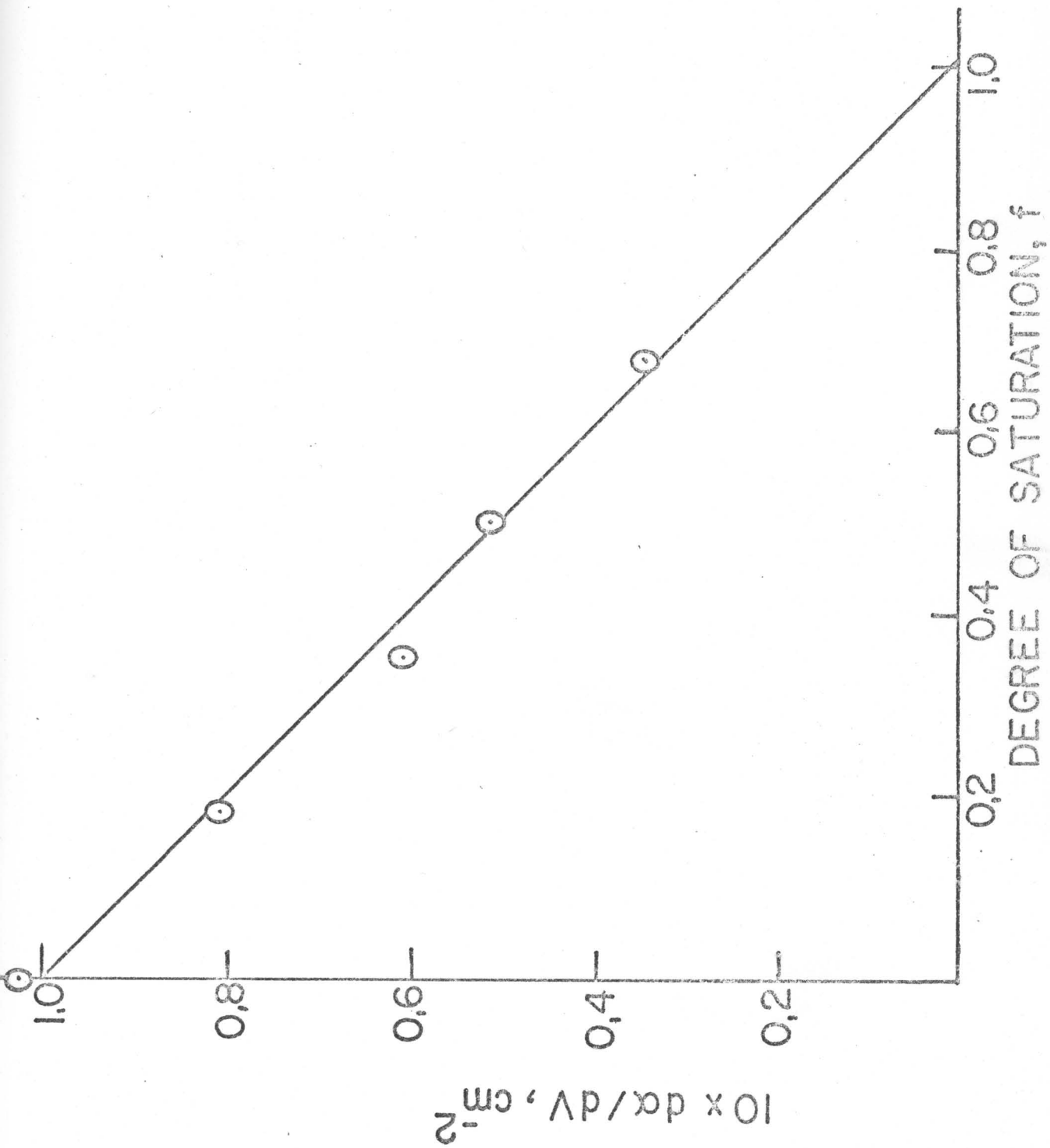
10 x dα/dV , cm⁻²
1.0
0.8
0.6
0.4
0.2
0.2
0.4
0.6
0.8
1.0
DEGREE OF SATURATION, f

Fig.24: $d\alpha/dV = \beta$ as a function of 'f' for -40/+60 mesh particles.

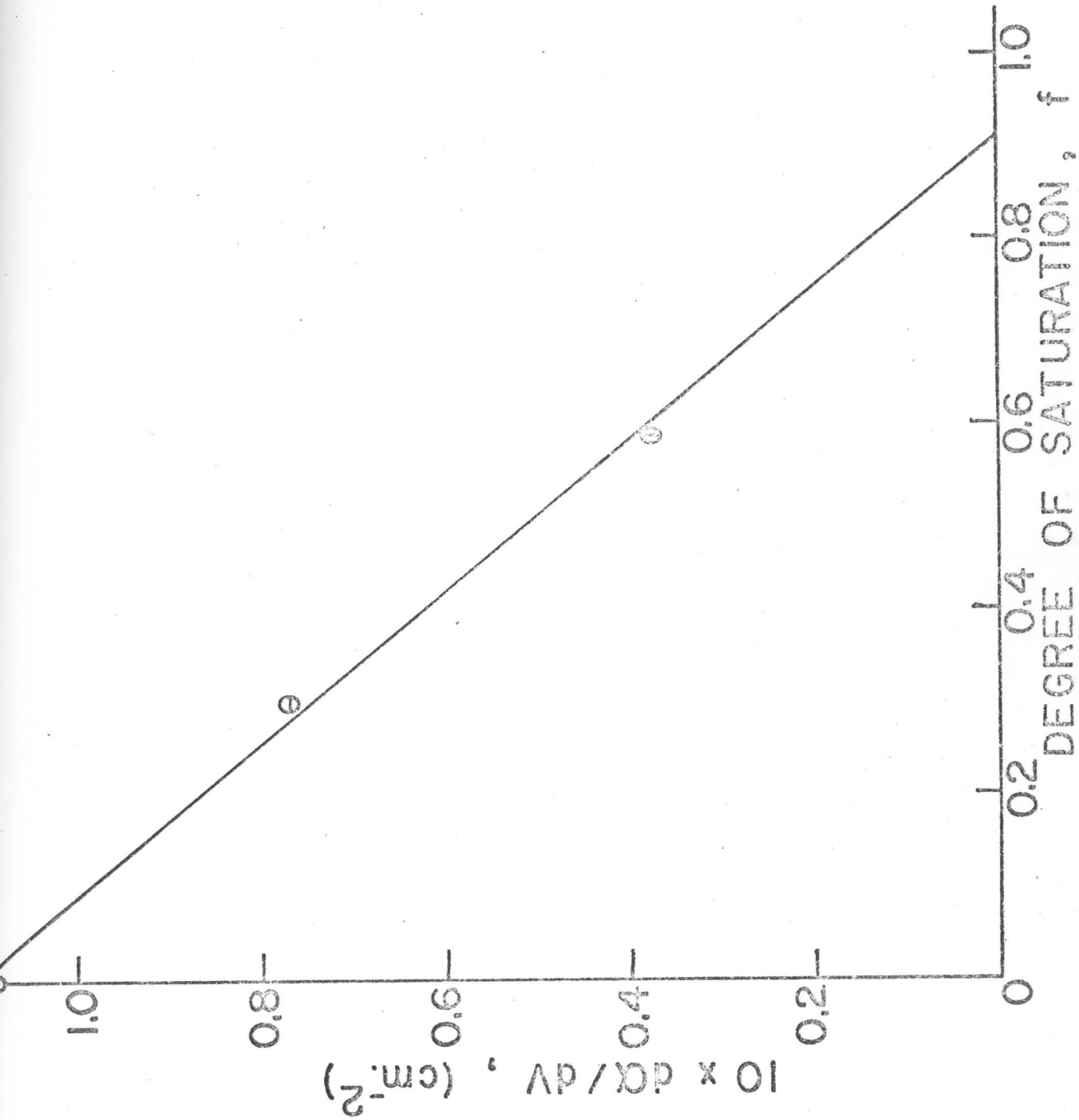
10 x dα/dv , (cm⁻²)
0.2
0.4
0.6
0.8
1.0
0
0.2
0.4
0.6
0.8
1.0
DEGREE OF SATURATION, f

It is noted from Figs. 23 & 24 that the plots are fairly linear and cut the f-axis close to f = q = 1 in accordance with Eq. 13. The slopes in Figs. 23 & 24 are -0.1.

Making reference to Fig. 19 and using the terminology of this figure, it is noted that a volume element Ωdx which is x cm. from the top of the column contains solid with a surface area of $A_x dx$, so that the dissolution rate in this volume element would be:

$$k \cdot A_x dx \cdot (S - C_x) \qquad \text{(Eq.14)}$$

Hence the dissolution rate over the entire column at time 't' when the length is ℓ cm. is:

$$-dm/dt = \int_0^{\ell} k \cdot A_x \cdot (S - C_x) \cdot dx \qquad \text{(Eq.15)}$$

The results from the experimental determination of A_x versus 'x' are shown in Fig.25. It would appear (as expected)[k]

---

[k] Examplewise, the number of particles of diameter d_1 in a single layer (d_1 cm. thick) is Ω/d_1^2, assuming a 'square' packing. The solid surface area is then $[\Omega/d_1^2]\pi d_1^2 = \pi\Omega$, so that the area per column length is $A_1 = \pi\Omega/d_1$. If, after some dissolution the diameter decreases to d_2, then by a similar argument $A_2 = \pi\Omega/(d_2) > A_1$ (because $d_2 < d_1$).

Fig.25: Surface area per cm. column length, A_x, is plotted as a function of distance, x, after a dissolution experiment for a -10/+20 mesh particle sample.

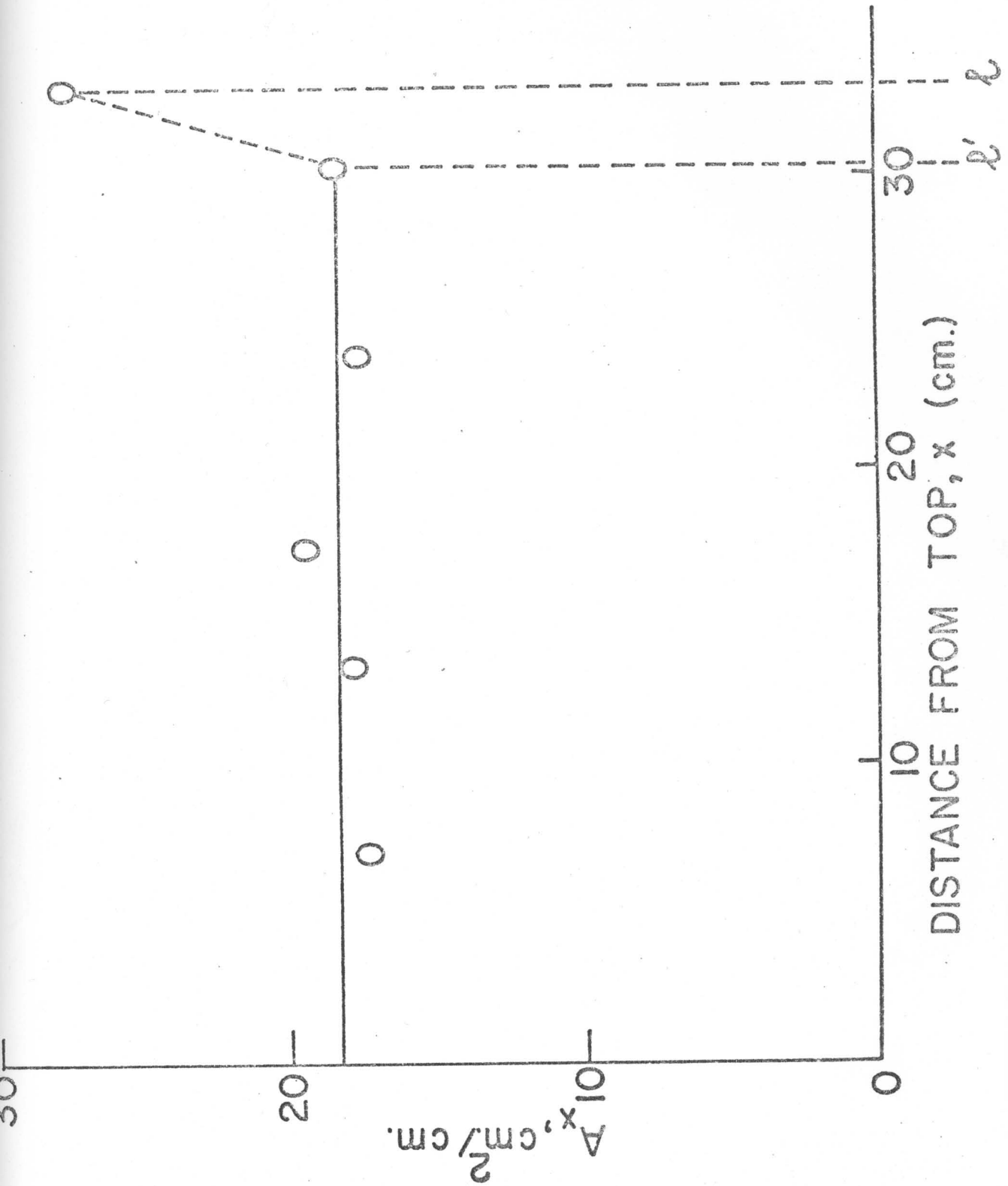
A_x, cm^2/ cm.
0
10
20
30
DISTANCE FROM TOP, x (cm.)
10
20
30
ℓ'
ℓ

that at the bottom of the solid column, A_x is high and then rapidly drops to a constant value. This drop occurs over a length of less than 3cm. (i.e. less than 10% of the length of the column); A_x is, hence, given by the expressions:

$$A_x = A_o \qquad x < \ell' \qquad \text{(Eq.16A)}$$

$$A_x = A_o + \varsigma(x-\ell') \qquad \ell' < x \leq \ell \qquad \text{(Eq.16B)}$$

where ℓ' as shown in Fig. 25, is the point where A_x starts increasing (and is close to ℓ, the total length of the column). Entering this into Eq.15 then gives:

$$-dm/dt = kA_o\int_0^{\ell}(S-C_x)dx + k\int_{\ell'}^{\ell}\varsigma(x-\ell')(S-C_x)dx \qquad \text{(Eq.17)}$$

The concentration profile of oxalic acid along the column length was determined and is shown in Fig.26. The slope of the curve suggests that (with real particles in real packings as opposed to hypothetical spheres with theoretical porosities) the concentration C_x is a function of x by the relation:

$$\ln\left[1-\frac{C_x-C_\ell}{S-C_\ell}\right] = gx + j \qquad \text{(Eq.18)}$$

as shown in Fig.27.

Fig. 26: $(C_x - C_\ell)/(S - C_\ell)$ is plotted as a function of distance, x, for a -20/+40 mesh particle sample. C_x is the concentration of oxalic acid in the column at distance x, C_ℓ is the concentration of oxalic acid in the feed liquid and 'S' is the solubility of oxalic acid in N/10 hydrochloric acid solution.

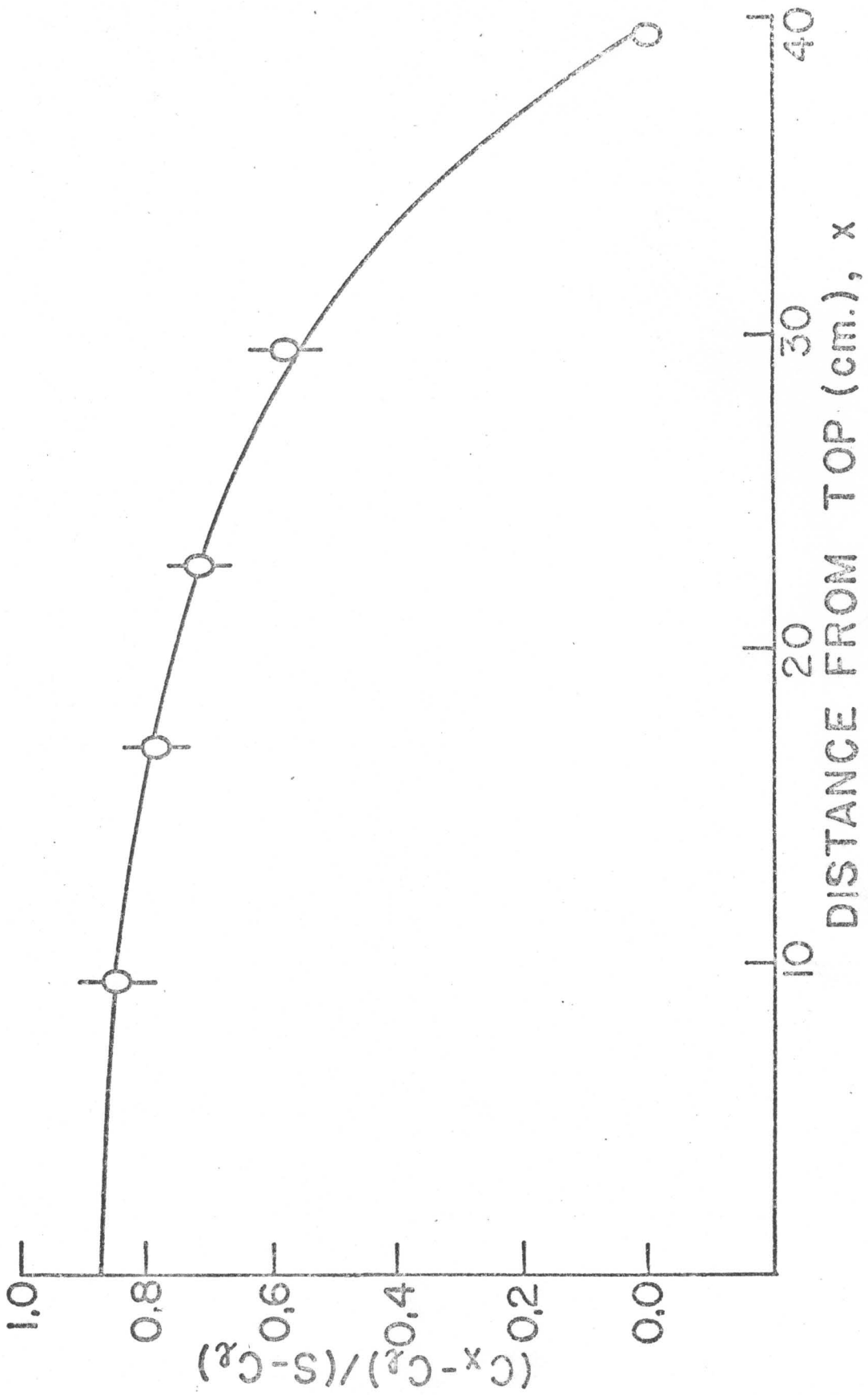
1.0
0.8
0.6
0.4
0.2
0.0
$(C_x-C_g)/(S-C_g)$
10
20
30
40
DISTANCE FROM TOP (cm.), x

Fig. 27: $\log \left[1-\left\{(C_x-C_\ell)/(S-C_\ell)\right\}\right]$ is plotted as a function of distance from top, x, for a -20/+40 mesh particle sample.
C_x is the concentration of oxalic acid in the column at distance x, C_ℓ is the concentration of oxalic acid in the feed liquid and S is the solubility of oxalic acid in N/10 hydrochloric acid solution.

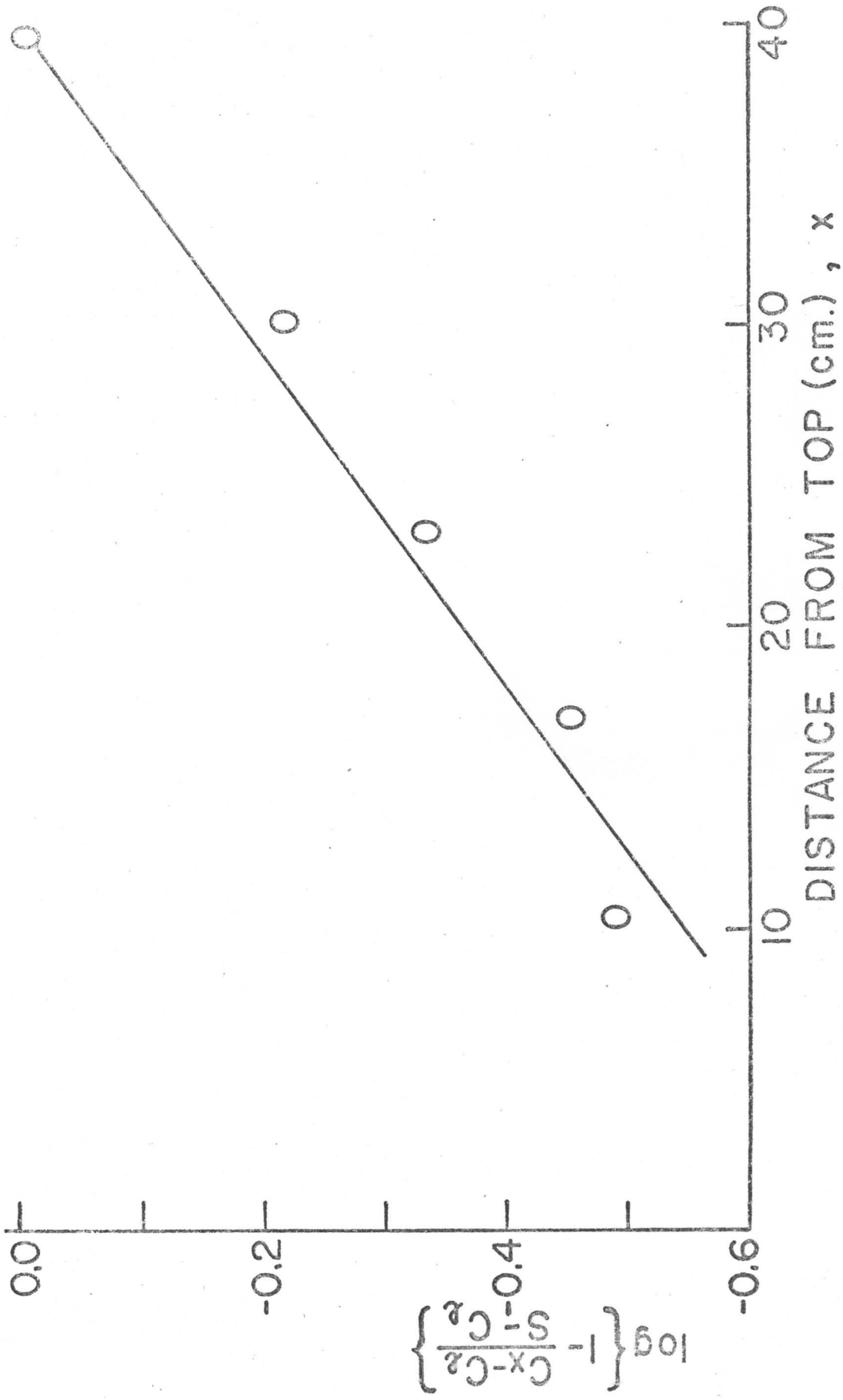
0.0
-0.2
-0.4
-0.6
10
20
30
40
DISTANCE FROM TOP (cm.), x
$\log\left\{1-\frac{C_x-C_e}{S-C_e}\right\}$

Introducing C_o (concentration at the top of the column) = Sq and C_ℓ (concentration at the bottom of the column) = Sf, this nay be written (as shown in Appendix I):

$$S-C_x = S(1-f)\cdot e^{g(x-\ell)} \qquad \text{(Eq.19)}$$

where: $$g = \frac{1}{\ell} \ln\left[(1-f)/(1-q)\right] \qquad \text{(Eq.20)}$$

Introducing Eq.19 into Eq.17 gives:

$$-dm/dt = \frac{kA_oS(1-f)}{g\cdot e^{g\ell}}(e^{g\ell}-1) + \frac{k\varepsilon S(1-f)}{g^2\cdot e^{g\ell}}(g\ell e^{g\ell} - e^{g\ell} -$$

$$g\ell' e^{g\ell'} + e^{g\ell'}) - \frac{k\varepsilon S\ell'(1-f)}{g\cdot e^{g\ell}}(e^{g\ell} - e^{g\ell'}) \qquad \text{(Eq.21)}$$

As mentioned, in the experimental data $\ell' \sim \ell$, sufficiently so as to allow to equate $e^{g\ell'}$ to $e^{g\ell}$, in which case Eq.21 can be simplified to (as shown in Appendix II):

$$-dm/dt = \frac{kA_oS\ell(q-f)}{\ln\left[(1-f)/(1-q)\right]} \qquad \text{(Eq.22)}$$

The rate constants were calculated according to Eq.22 for all the conditions used. When the experimental values of k (cm./sec.) obtained in this fashion were plotted as a function of velocity (c.c./sec.), linear plots result with the following least squares fit equations:

Mesh size	Equation	
-10/+20	$k = (7.45 \cdot 10^{-4}) \cdot V + (4.03 \cdot 10^{-4})$	(Eq.23)
-20/+40	$k = (4.76 \cdot 10^{-4}) \cdot V + (-0.31 \cdot 10^{-4})$	(Eq.24)
-40/+60	$k = (6.57 \cdot 10^{-4}) \cdot V + (-4.18 \cdot 10^{-4})$	(Eq.25)

Then 95% confidence intervals on intercepts were calculated and it was found that they do not differ significantly from zero. Therefore all the data have been pooled and are shown in Fig. 28. The confined least squares fit is:

$$k = (6.48 \pm 0.07) \cdot 10^{-4} \cdot V \qquad \text{(Eq.26)}$$

where $(0.07 \cdot 10^{-4})$ is the 95% confidence interval on the slope. The lengths of the bars in Fig. 28 are 95% confidence intervals calculated conventionally (one example is shown in Table VII) according to $\gamma = t_{n-1,0.05}\frac{\sigma}{\sqrt{n}}$, where $\sigma/\sqrt{n}$ is the standard error and $t_{n-1,0.05}$ is the Student t-value for (n-1) degrees of freedom.

It is shown below that the liquid velocity is of a magnitude dictating laminar (or slightly turbulent) flow. This is presumably the type of flow around a particle in most dissolution methods. Extrapolation to zero velocity is possible via Eq. 23 to 25. Carstensen and Patel (15)

Fig. 28: Dissolution rate constants, k (cm./sec.) as a function of liquid flow rate, V (c.c./sec.) plot.

⊙ : f = 0.0 , -10/+20 mesh particles.

◐ : f = 0.27, -10/+20 mesh particles.

⊖ : f = 0.61, -10/+20 mesh particles.

⊗ : f = 0.0 , -20/+40 mesh particles.

⊡ : f = 0.18, -20/+40 mesh particles.

◫ : f = 0.35, -20/+40 mesh particles.

⊟ : f = 0.52, -20/+40 mesh particles.

⊠ : f = 0.68, -20/+40 mesh particles.

◬ : f = 0.0 , -40/+60 mesh particles.

△ : f = 0.30, -40/+60 mesh particles.

△ : f = 0.59, -40/+60 mesh particles.

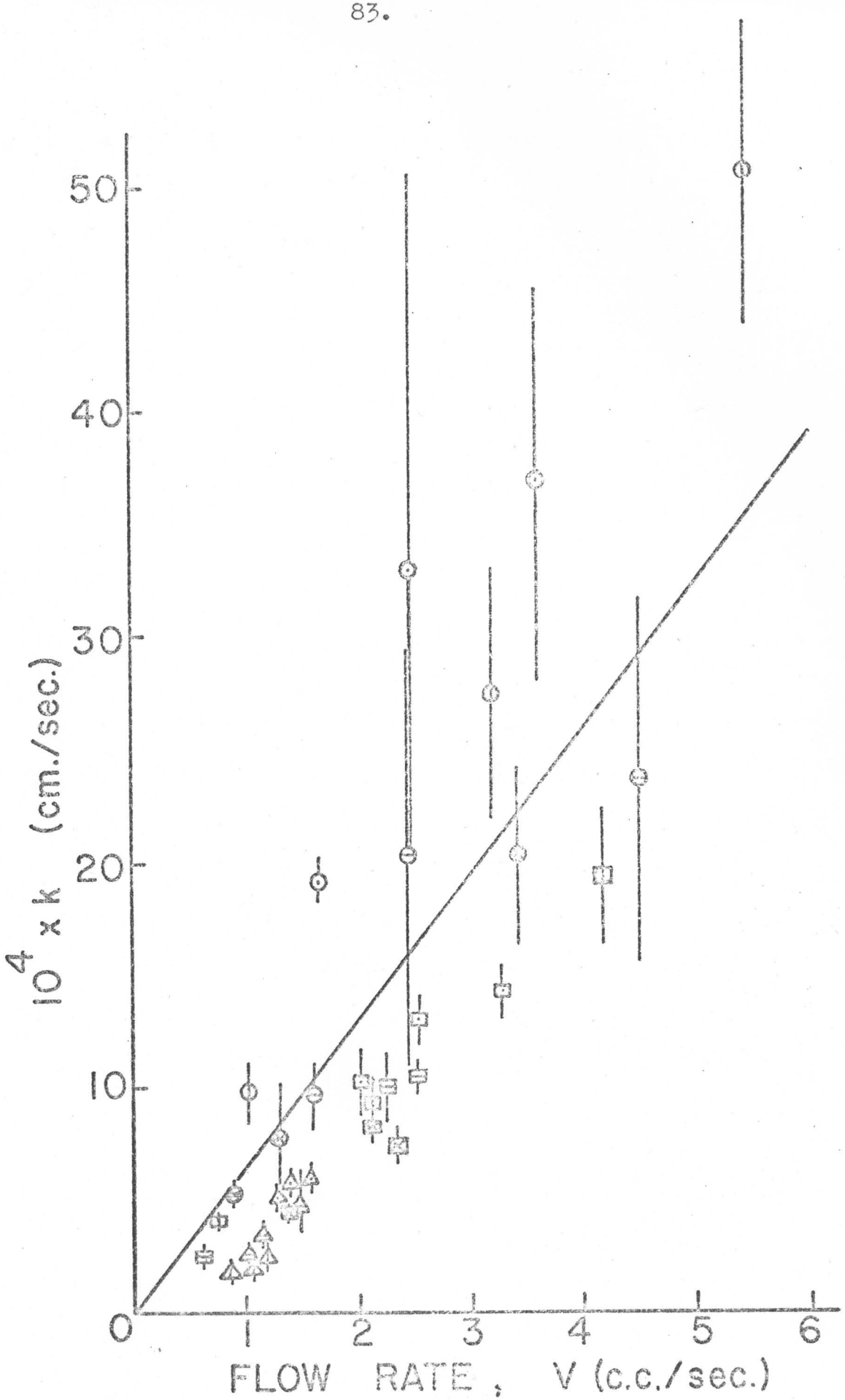
50
40
30
20
10
0
1
2
3
4
5
6
$10^4 \times k$ (cm./sec.)
FLOW RATE, V (c.c./sec.)

Table VII: V (c.c./sec.) versus k (cm./sec.) values calculated according to Eq. 22 for a -10/+20 mesh sample.

	V(c.c./sec.)	$10^4 \cdot k$ (cm./sec.)
	0.94	9.35
	1.04	9.44
	0.99	9.32
	1.11	10.91
Average =	1.02	9.76
$t_{3,0.05}$ =	-	3.18
σ =	-	0.77
$t_{3,0.05} \cdot \sigma/\sqrt{n} = \gamma$ =	-	1.23

have shown that static dissolution rate constants are at least an order of magnitude smaller than those found from 'usual' beaker type dissolution rate methods. For example, for a flow rate, used here, of the order of 2c.c./sec., a column cross-section of 0.93 $cm.^2$ and a porosity of 0.4 would give a linear flow velocity of $2/(0.4 \cdot 0.93) = 5.38$ cm./sec. For a 20 mesh particle, the diameter is d = 0.084 cm. so that the Reynolds number (calculated according to Levich (18,19))is $Re = v \cdot d \cdot \phi/\eta$ where ϕ (gm./c.c.) and η (poise) are the density and viscosity of the liquid used respectively. Assuming values of these to be $\phi = 1.0$ g./c.c. and $\eta = 0.01$ Poise gives $Re = (5.38 \cdot 0.084 \cdot 1.0)/0.01 = 45$. Groves et. al. (20) in column work (with tablets) found backflow at $Re < 10$ and instability at $Re > 100$. In Fig.28 it is observed that the length of the bars is large in cases of -10/+20 mesh particle samples where flow rate is larger than 1.86 c.c./sec. ($Re > 100$).

A fair amount of work has been reported on the use (or potential use) of column apparatuses for dissolution of dosage forms (7,16,21-28). The film theory type of equations have been found to hold in many cases (24,28).

The work reported here does <u>not</u> intend to describe another dissolution method with application to dosage forms. The apparatus was constructed because it appears to be the best way of creating well defined linear liquid

velocities, and the sole intent of its construction was to study the dissolution of an easily reproducible crystal. In the process the equation for dissolution of a dissolving powder in a column type operation have been derived. Mass transport equations for column apparatus have appeared in literature (29) but mostly relating to solid supports (which adsorb and desorb solutes from and into the feed but which themselves remain of constant weight) and non-disintegrating entities (24). Actual dissolution in columns has been reported on occasion (30) but in these cases at high Reynolds numbers (100-1000).

Oxalic acid was used in this study because it has been shown (15) to be easily reproducible in fairly coarse particle size, and it remains isometric during dissolution so that the general film theory type equations hold during its dissolution at low Reynolds numbers.

The experiments were carried out at a series of temperatures; the k-values obtained are plotted as (k/T) versus 1/T and according to Puisieux and Carstensen (31) should be linear with slopes between E_η and $2E_\eta$, where E_η is the energy of activation of the viscosity of the dissolving liquid. That this is the case is seen in Fig. 29. It is noted from the figure that oxalic acid dihydrate has a dissolution rate constant which can be represented by the

Fig.29: Plot of (k/T) as a function of reciprocal absolute temperature. E_a = 3950 cal./mole.

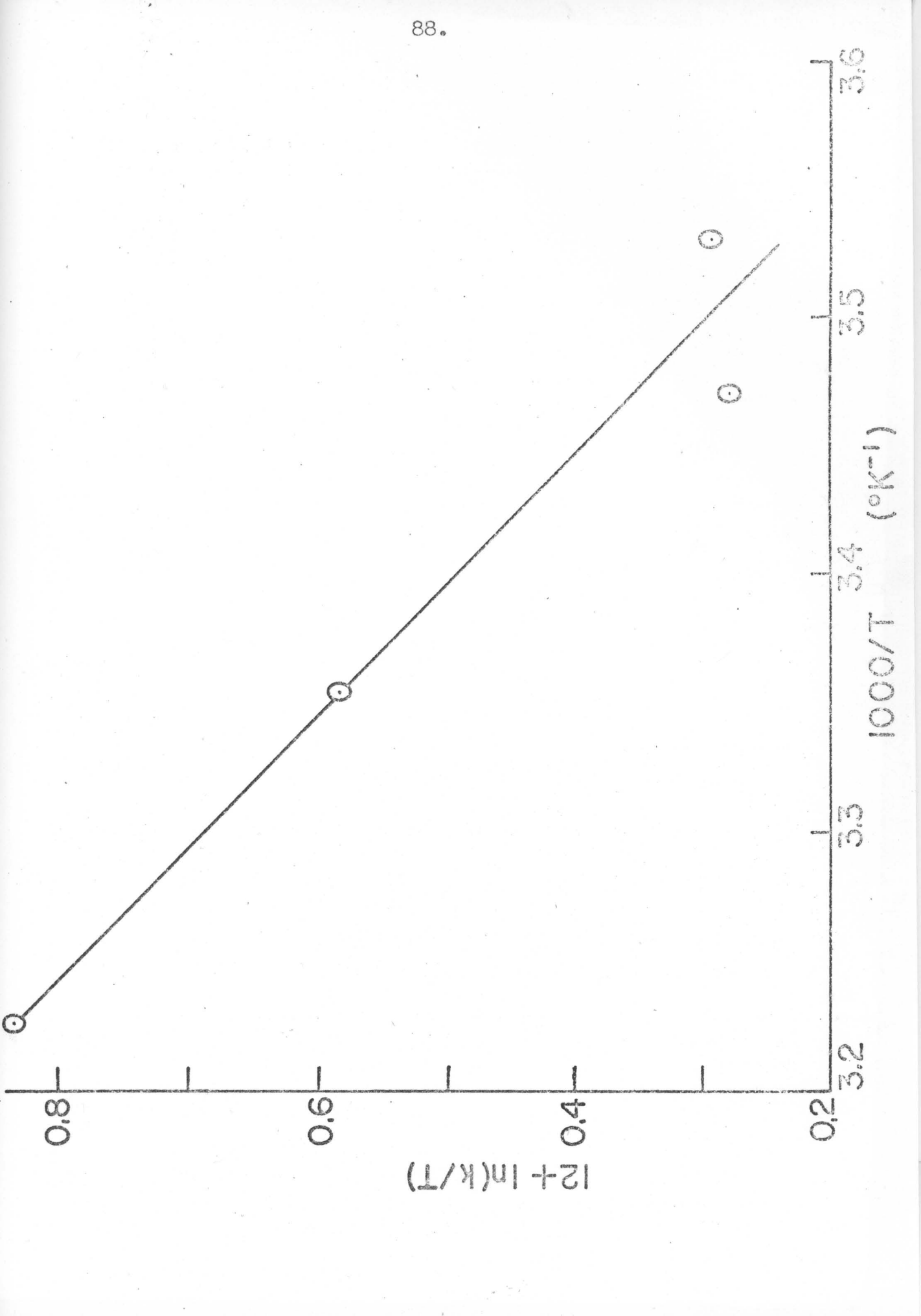
12+ ln(k/T)
0.8
0.6
0.4
0.2
3.2
3.3
3.4
3.5
3.6
1000/T (°K⁻¹)

following eqution:

$$\ln (k/T) = -(1988/T) - 4.75 \qquad \text{(Eq.27)}$$

This gives an activation energy of $E_a = R \cdot 1988 = 3950$ cal./mole , which is close to the activation energy of water (4000 cal./mole).

The least squares fit equations shown in Eqns. 23 to 25 have been made with flow rate, V (c.c./sec.) as the independent variable and the intercept values are shown not to differ significantly from zero. The flow rates, V (c.c./sec.) have been converted to liquid velocities, $\bar{v}$ (cm./sec.) via Eq.9. The least squares fit equations of k (cm./sec.) vs. $\bar{v}$ (cm./sec.) are confined to zero intercept (i.e., slope = $\Sigma xy / (\Sigma x^2)$). The slopes and the 95% confidence limits of the slopes calculated in this fashion are shown in Table VIII.

It is expected that k-values should be a function of $\bar{v}$ (cm./sec.) and, indeed, at smaller particle sizes they are (11). The studies here fail to show significant differences at the coarse particle sizes tested as shown in Table VIII. The last line gives the composite value of all the mesh fractions tested, i.e., oxalic acid dihydrate has a dissolution rate constant which can be represented by the equation:

Table VIII: Slopes of k(cm./sec.) vs. $\bar{v}$(cm./sec.) plots.

Mesh fraction	Slopes (10^4)	95% confidence limits on slope (10^4)	Degrees of freedom
-10/+20	3.67	0.31	8
-20/+40	1.79	0.007	14
-40/+60	1.28	0.03	8
Composite	2.58	0.01	32

$$k = (2.58 \pm 0.01) \cdot 10^{-4} \cdot \bar{v} \qquad \text{(Eq.28)}$$

where k is in cm./sec. and $\bar{v}$ is in cm./sec.

This can be used in a practical sense to calculate the 'average velocity', $\bar{v}$ (and from this the Reynolds number) of a dissolution test or a particular piece of equipment; this is done in the following fashion: oxalic acid dihydrate is prepared by recrystallization from water and dried at room temperature and atmospheric pressure to constant weight. Its stoichiometric composition is verified by base titration or permanganometry. A sieve fraction of upper limit of less than or equal to 10 mesh and a lower limit of 60 mesh or higher is sieved off. A microscopic particle size measurement is carried out and the specific geometric surface area, A' $cm.^2/gm.$, calculated. m_o g. of the sample is subjected to a dissolution test in the specific apparatus or piece of equipment that is being tested for 'average velocity'. The initial dissolution rate is given by:

$$dm/dt = k \cdot A' \cdot m_o \cdot S \qquad \text{(Eq.29)}$$

from which k is found. It is noted that if S is in mg./c.c. then m_o is in mg.; and if S is in g./c.c., then m_o is in gm. t is measured in seconds. The calculated value of

k (cm./sec.) is then inserted in Eq. 28 and the value of $\bar{v}$ (cm./sec.) calculated.

It should be recalled (32,33,34) that t_{90} , t_{50} or other parameter points of a dissolution procedure depend partly on how the dissolution rate apparatus works as a disintegrating device. Most dissolution rate curves of tablets are of the type:

$$\ln\left[(M/Q)-C\right] = -K(t-t_i) + \ln(M/Q) \qquad \text{(Eq.30)}$$

where M is the amount of active substance in the tablets tested, Q is the dissolution volume, C is the concentration of the active substance in the dissolution liquid, K is a dissolution constant which is a function of k and where the lag time, t_i, is a function of how well the dissolution rate apparatus works as a disintegration apparatus. The value of K (but not t_i) is therefore related to $\bar{v}$.

It has become more and more apparent lately that there are frequent instrument-to-instrument differences, laboratory-to-laboratory differences and operator-to-operator differences. For example, it has been reported (34) that the wabbling of the shaft in the U.S.P. basket apparatus gives rise to considerable variation in results. An example of a recent comparison of methods is the report

by Needham and Luzzi (35). Here the U.S.P. method, the modified Levy method (36-38) and the magnetic basket method (39,40) were compared to see if results differed. The hydrodynamics were different, and as expected the tests showed a significant method-to-method difference. They did not show capsule-to-capsule (or tablet-to-tablet) differences within the individual tests. This demonstrates the integrety of such methods by themselves and the oxalic acid dihydrate (or other similar substance) could be used to correlate results from different methods. When different pieces of equipment of the same construction design are used, however, piece-to-piece differences are often substantial, as recently reported in a comprehensive study of the U.S.P. dissolution test by Knapp (3). Since hydrodynamic parameters are very sensitive to geometry and such (seemingly unimportant) parameters as shaft position (6) and wabble, it might be worthwhile considering internal standards for such tests. The study reported here shows that oxalic acid dihydrate has the following properties which makes the rationale for an internal standard sound: (a) the dissolution rate constant is proportional to the magnitude of the liquid velocity, (b) it is easily recrystallised and (c) the geometric surface area can be used. This latter point is, essentially, a flaw, since the area term in Eq.29 ($m_o A'$) is not a true surface area

the rugosity of fractions between 10 and 60 mesh, however, appear to be sufficiently constant, so that the geometric surface area is proportional to the real surface area. The rate constants reported here, and Eq.16, hence refer to geometric surface areas. A practical approach to the use of oxalic acid dihydrate as an internal standard would be to make oxalic acid tablets (of the same dimensions as the actual tablets to be tested) and ascertain that dissolution (and no disintegration) took place from the compressed surface. This approach assumes that a compressed mass has the same k-value as a single crystal.

APPENDIX I

Eq. 18 may be written as:

$$1 - \left[(C_x - C_\ell)/(S - C_\ell)\right] = (S - C_x)/(S - C_\ell) = A \cdot e^{gx} \qquad \text{(Eq.AI-1)}$$

where $A = e^{j}$ (Eq.AI-2)

Eq.AI-1 may be written:

$$C_x = S - (S - C_\ell) \cdot A e^{gx} \qquad \text{(Eq.AI-3)}$$

At $x = \ell$, $C = S \cdot f$, so:

$$S \cdot f = S - (S - Sf) \cdot A \cdot e^{g\ell} \qquad \text{(Eq.AI-4)}$$

i.e., $A = e^{-g\ell}$. Inserting this, and $C_o = Sq$ at $x=0$ in Eq.AI-3 gives:

$$C_o = S \cdot q = S - S(1-f) \cdot e^{-g\ell} \qquad \text{(Eq.AI-5)}$$

or $S(1-q) = S(1-f)\, e^{-g\ell}$ (Eq.AI-6)

Hence: $e^{g\ell} = \left[(1-f)/(1-q)\right]$ (Eq.AI-7)

i.e., $$g = \frac{1}{\ell} \ln\left[(1-f)/(1-q)\right] \qquad \text{(Eq.AI-8)}$$

The complete equation, then is:

$$C_x = S - (S-Sf)\cdot e^{g(x-\ell)} \qquad \text{(Eq.AI-9)}$$

or, $$S - C_x = S(1-f)\cdot e^{g(x-\ell)} \qquad \text{(Eq.AI-10)}$$

APPENDIX II

Inserting Eq.19 into Eq.17 gives:

$$-dm/dt = kA_o\int_o^{\ell} S(1-f)e^{g(x-\ell)}dx + k\int_{\ell'}^{\ell} \xi(x-\ell')S(1-f)e^{g(x-\ell)}dx \qquad \text{(Eq.AII-1)}$$

$$\text{or, } -\frac{dm}{dt} = kA_o\frac{S(1-f)}{e^{g\ell}}\int_o^{\ell} e^{gx}dx + k\xi\frac{S(1-f)}{e^{g\ell}}\int_{\ell'}^{\ell} xe^{gx}dx$$

$$- k\xi\ell'\frac{S(1-f)}{e^{g\ell}}\int_{\ell'}^{\ell} e^{gx}dx \qquad \text{(Eq.AII-2)}$$

The substitution $u = gx$ ($dx = \frac{1}{g}du$) is then made with the appropriate change in the limits: for $x = 0$, $u = 0$ and for $x = \ell$, $u = g\ell$. Eq.AII-2 then becomes:

$$-dm/dt = kA_o\frac{S(1-f)}{g\cdot e^{g\ell}}\int_o^{g\ell} e^u du + k\xi\frac{S(1-f)}{g^2\cdot e^{g\ell}}\int_{g\ell'}^{g\ell} u\cdot e^u du$$

$$- k\xi\ell'\frac{S(1-f)}{g\cdot e^{g\ell}}\int_{g\ell'}^{g\ell} e^u du \qquad \text{(Eq.AII-3)}$$

Noting that $\int ue^u du = ue^u - e^u$ + integration constant, then Eq.AII-3 expands into:

$$-\frac{dm}{dt} = kA_o\frac{S(1-f)}{g\cdot e^{g\ell}}(e^{g\ell}-1) + k\xi\frac{S(1-f)}{g^2 e^{g\ell}}(g\ell e^{g\ell} - e^{g\ell} - g\ell'\cdot e^{g\ell'}$$

$$+ e^{g\ell'}) - k\xi\ell'\frac{S(1-f)}{g\cdot e^{g\ell}}(e^{g\ell} - e^{g\ell'}) \qquad \text{(Eq.AII-4)}$$

With the assumption that $\ell \sim \ell'$ so that, also $e^{g\ell} \sim e^{g\ell'}$, the last two terms vanish, and the equation may be written:

$$-dm/dt = kA_o \frac{S(1-f)}{g \cdot e^{g\ell}} (e^{g\ell} - 1) \qquad \text{(Eq.AII-5)}$$

introducing Eq.20, this then becomes:

$$-\frac{dm}{dt} = \frac{kA_oS(1-f)\cdot\ell}{\ln(\frac{1-f}{1-q})\cdot\left[\exp.(\ln \frac{1-f}{1-q})\right]} \left[\left\{\exp.(\ln \frac{1-f}{1-q})\right\} - 1\right] \qquad \text{(Eq.AII-6)}$$

Therefore:

$$-dm/dt = \frac{kA_oS\ell\cdot(q-f)}{\ln(\frac{1-f}{1-q})} \qquad \text{(Eq.AII-7)}$$

REFERENCES

(1) Pernarowski, M., "Dissolution Technology", IPT of Acad. Pharm. Sci., Washington, D.C., 1974, pg.58.

(2) LeHir, A., Colloque Pharmaceutique International, Montpellier, pg. 1-34 (1972).

(3) Knapp, G.G., U.S.P. Open Conf., June 13, 1975, Washington, D.C.

(4) Beyer, W.F. and Smith, D.L., J.Pharm. Sci. 60, 496 (1971).

(5) Mattock, G.L.,McGilveray, I.J. and Hossie, R.D., J.Pharm. Sci., 61, 460 (1972).

(6) Desta, B. and Pernarowski, M., J.Pharm. Sci., 62, 1029 (1973).

(7) Whithey, R.J. and Bowker, A.J., J.Pharm.Pharmacology, 24, 346 (1972).

(8) Nernst,W., Z.Phys.Chem., 47, 52 (1904).

(9) Brunner, E., Z.Phys.Chem., 51, 95 (1905).

(10) Wagner, J., J.Pharm. Sci. 50, 359 (1961).

(11) Niebergall, P.J., Milsovich, G. and Goyan, J.E., J.Pharm.Sci., 52, 236 (1963).

(12) Nelson, K. and Shah,A.C.,Abstracts, 17th. National Meeting of A.Ph.A. Acad. of Pharm.Sci., New Orleans, Nov. 10-14, 1974, 4 (2), 138 paper 70.

(13) Shah, A.C. and Nelson, K.G., ibid., 4 (2), 138 paper 71.

(14) Wood, J.H., Syrato, J.E. and Letterman, H., J.Pharm.Sci., 64, 1068 (1965).

(15) Carstensen, J.T. and Patel, M., J.Pharm.Sci., 64, 1770 74, 1651 (1975). ← wrong ref?!

(16) Tingstad, J., Dudzinski, J., Lachman, J. and Shami, E, J.Pharm.Sci., 62, 1527 (1973).

(17) Gray, W.A.: "The Packing of Solid Particles", Chapman and Hall, Ltd., London, 1968, pg.129.

(18) Levich, V.G.: "Physicochemical Hydrodynamics", Prentice Hall Inc., Englewood Cliffs, 1962, pg.7.

(19) Langenbucher, F., Pharm.Acta Helv., 49, 187 (1974).

(20) Groves, M.J., Alkan, M.H. and Deer, M.A., J.Pharm. Pharmacology, 27, 400 (1975).

(21) Tingstad, J.E. and Riegelman, S., J.Pharm.Sci., 59, 692 (1970).

(22) Tingstad, J.E., Gropper, E., Lachman, L. and Shami, E., J.Pharm.Sci. 61, 1985 (1972).

(23) Tingstad, J.E., Gropper, E., Lachman, L. and Shami, E., J.Pharm.Sci., 62, 293 (1973).

(24) Langenbucher, F., J.Pharm.Sci., 58, 1265 (1969).

(25) Marshall, K. and Brook, D.B., J.Pharm. Pharmacology, 21, 790 (1969).

(26) Baun, D.C. and Walker, G.C., J.Pharm.Sci., 58, 611 (1969).

(27) Lark, C.F. and Zuurman, K., J.Pharm.Pharmacology, 22, 319 (1970).

(28) Richter, A., Myhre, R. and Khama, S.C., J.Pharm. Pharmacology, 21, 409 (1969).

(29) Ergun, S., Chem.Eng.Progress, 48, 227 (1952).

(30) Mullen, J.W. and Cook, T.P., J.Appl.Chem., 15, 145 (1965).

(31) Pusieux, F. and Carstensen, J.T., Accepted for Publication, Annales Pharmaceutiques Francaises.

(32) Carstensen, J.T.: "Pharmaceutics of Solids", Badger Freund Inc., Fond du Lac, WI, 1974, pg. 89.

(33) Johnson, J.B., Kennedy, P.G. and Rubin, S.H., J.Pharm. Sci., 63, 1931 (1974).

(34) Madan, P.L., J.Pharm.Sci., 64, 1080 (1975).

(35) Needham, T.E. and Luzzi, L.A., J.Pharm.Sci., 63, 925 (1974).

(36) Levy, G. and Hayes, B.A., New Engl. J.Medicine, 262, 1053,(1960).

(37) Levy, G., J.Pharm.Sci., 52, 1039 (1963).

(38) Levy, G. and Sahli, B., J.Pharm.Sci.,51, 58 (1962).

(39) Needham, T.E., Shepherd, R.E. and Luzzi, L.A., J.Pharm.Sci., 63, 470 (1973).

(40) Shepherd, R.E., Price, J.C. and Luzzi, L.A., J.Pharm.Sci., 61, 1152 (1972).

(41) King, C.V., J.Amer.Chem.Soc., 57, 828 (1935).